



**UNIVERSITAT POLITÈCNICA DE CATALUNYA**  
**BARCELONATECH**

---

**Escola Tècnica Superior d'Enginyeria  
de Telecomunicació de Barcelona**

**“RED PITAYA CONTROLLED TUNEABLE SEMICONDUCTOR  
LASER”**

A MASTER'S THESIS

SUBMITTED TO THE FACULTY OF

**ESCOLA TÈCNICA D'ENGINYERIA DE TELECOMUNICACIÓ DE BARCELONA**

**UNIVERSITAT POLITÈCNICA DE CATALUNYA**

BY

**SANDOVAL GALIANA DAVID GUILLERMO**

IN PARTIAL FULFILLMENT

OF THE REQUIREMENTS FOR THE DEGREE OF

**MASTER IN ELECTRONIC ENGINEERING**

ADVISOR

**LAZARO VILLA JOSE ANTONIO**

**BARCELONA, JULY 2018**



**TITLE OF THE THESIS:** Red Pitaya controlled tuneable semiconductor laser

**AUTHOR:** David Guillermo Sandoval Galiana

**ADVISOR:** José Antonio Lázaro Villa

## **ABSTRACT**

This master's thesis has been focused on the design, manufacture and characterization of a compact conditioning circuit, controlled by Red Pitaya, to tune a Grating Coupled Sampled Reflector (GCSR) laser.

First, a bibliographic study about GCSR laser characteristics and current control requirements for its use was done.

Second, the use of Red Pitaya for controlling current sources, for power and wavelength monitoring was analysed.

Third, the circuit was designed and experimental verification was performed in the laboratory. The response of the complete system, laser and circuit was analysed to see if it corresponds to the laser characterization, and modifications were done to obtain it.

Fourth, the PCB circuit with the modifications was fabricated and the response of the complete system was analysed.

Finally, future lines are proposed to improve the functioning of the device.

## ACKNOWLEDGMENTS

I want to give thanks to my director José Antonio Lazaro Villa, for giving me the opportunity to do this project, for his support and good advice throughout the work. Many thanks to my companions Kevin Sacco, Carlos March, María Victoria Ortiz and Santiago Córdoba, for making the master's degree a good experience and for making me the person that I am now.

Special thanks to my friends Xavier Botines, Nàdia Maldonado, José Carlos Guillén, Joe Hidalgo, Cuauhtémoc Salazar, Cindy Avalos and Johanna Kais, who have always been by my side listening to me, supporting me, and giving me those moments of disconnection from work.

And of course, many thanks to my mom, my dad and my sisters, for their unconditional support, for sharing my successes and failures, for giving me the best education a son can desire, and above all, for the effort that they have made so that I could be here.

## REVISION HISTORY AND APPROVAL RECORD

Revision	Date	Purpose
0	07/07/2018	Document creation
1	11/07/2018	Document revision

Written by:		Reviewed and approved by:	
Date	07/07/2018	Date	17/07/2018
Name	David Guillermo Sandoval Galiana	Name	José Antonio Lázaro Villa
Position	Project Author	Position	Project Supervisor

## INDEX

<b>ABSTRACT</b>	<b>i</b>
<b>ACKNOWLEDGEMENTS</b>	<b>ii</b>
<b>REVISION HISTORY AND APPROVAL RECORD</b>	<b>iii</b>
<b>LIST OF FIGURES</b>	<b>vi</b>
<b>LIST OF TABLES</b>	<b>viii</b>
<b>CHAPTER 1 INTRODUCTION</b>	<b>1</b>
1.1 Project overview	1
1.2 Project goals	1
1.3 Requirements and specifications	2
<b>CHAPTER 2 STATE OF THE ART</b>	<b>3</b>
2.1 Semiconductor laser	3
2.1.1 Semiconductor laser architecture	3
2.2 Tuneable laser	6
2.3 GCSR laser	9
2.4 NYW 30-009 GCSR laser	10
2.4.1 Gain section	12
2.4.2 Coupler section	13
2.4.3 Reflector section	13
2.4.4 Phase section	14
2.4.5 Wavelength ranges and frequency efficiency	15
2.5 STEMLab Red Pitaya	15
<b>CHAPTER 3 PROJECT DEVELOPMENT</b>	<b>19</b>
3.1 Red Pitaya testing	19

3.2 Hardware	25
3.2.1 Hardware requirements	25
3.2.1.1 Voltage regulator with soft start	25
3.2.1.2 Current sources	30
3.2.1.3 Temperature controller	33
3.2.1.4 Optical measurement	39
3.2.2 Complete circuit	41
3.3 Input-output relationship	44
3.4 Software	44
3.4.1 Language selection	44
3.4.1.1 Matlab	44
3.4.1.2 Python	45
3.4.1.3 Summary	46
3.4.2 Matlab coding	47
 <b>CHAPTER 4 TESTING AND RESULTS</b>	 <b>50</b>
4.1 Assembling and running project	50
 <b>CHAPTER 5 BUDGET</b>	 <b>54</b>
 <b>CHAPTER 6 CONCLUSION AND FUTURE DEVELOPMENTS</b>	 <b>55</b>
 <b>BIBLIOGRAPHY</b>	 <b>56</b>
 <b>GLOSSARY</b>	 <b>58</b>

## LIST OF FIGURES

<b>Figure 1.</b> Fabry-Perot cavity laser	4
<b>Figure 2.</b> Wavelengths of the $i$ -th longitudinal mode	5
<b>Figure 3.</b> Schematic of a generic tunable laser	6
<b>Figure 4.</b> Examples of single-frequency lasers (not tunable): (a) DFB laser and (b) VCSEL	7
<b>Figure 5.</b> Examples of widely-tunable laser types: (a) selectable DFB array, (b) external cavity, (c) MEMs/VCSEL, (d) Grating-Coupled Sampled-Reflector (GCSR) and (e) sampled-grating DBR (SGDBR) with integrated SOA	8
<b>Figure 6.</b> Detail of the four sections of a GCSR laser with the wavelength path	9
<b>Figure 7.</b> NYW 30-009 ALTITUN GCSR laser in butterfly package	10
<b>Figure 8.</b> NYW 30-009 ALTITUN GCSR pin configuration	10
<b>Figure 9.</b> Power output versus gain current for a fixed coupler current of 10 mA, reflector current of 12.5 mA and a phase current of 0.3 mA at $T=25^{\circ}\text{C}$ [1].	12
<b>Figure 10.</b> Wavelength versus coupler section current for a fixed reflector current of 3 mA and phase current of 1 mA at $T=25^{\circ}\text{C}$ [1].	13
<b>Figure 11.</b> Reflector section current-wavelength characteristics for a fixed coupler current of 9.7 mA and phase current of 1 mA at $T=25^{\circ}\text{C}$ [1].	14
<b>Figure 12.</b> Phase section current-wavelength characteristics for a fixed coupler current of 11 mA and reflector current of 5 mA at $T=25^{\circ}\text{C}$ [1].	14
<b>Figure 13.</b> Wavelength and current ranges for each GCSR section at $T=25^{\circ}\text{C}$ [1].	15
<b>Figure 14.</b> Red Pitaya Ecosystem	16
<b>Figure 15.</b> Red Pitaya hardware overview	17
<b>Figure 16.</b> (a) Extension connector characteristics and (b) I/O pins location.	19
<b>Figure 17.</b> STEMLab main page	20
<b>Figure 18.</b> STEMLab network manager	21
<b>Figure 19.</b> Wireless connection established	21
<b>Figure 20.</b> SCPI connection	22
<b>Figure 21.</b> Testing of the analog output pins	23
<b>Figure 22.</b> Analog output error.	23
<b>Figure 23.</b> Testing of the analog input pins	24
<b>Figure 24.</b> ADC error	24



<b>Figure 25.</b> Positive and negative voltage regulator with soft start schematic.	26
<b>Figure 26.</b> Voltage regulator.	28
<b>Figure 27.</b> Voltage regulator with soft start.	28
<b>Figure 28.</b> Current source with feedback loop	30
<b>Figure 29.</b> Current sources for each GCSR laser section.	33
<b>Figure 30.</b> R-T curve of the thermistor.	34
<b>Figure 31.</b> Wheatstone bridge circuit	35
<b>Figure 32.</b> Voltage error	36
<b>Figure 33.</b> Proportional compensator	36
<b>Figure 34.</b> Derivative compensator	37
<b>Figure 35.</b> Integral compensator	37
<b>Figure 36.</b> PID controller	38
<b>Figure 37.</b> Darlington amplifier stage with current limit resistance and instrumentation amplifier	39
<b>Figure 38.</b> Inverting transimpedance stage measuring optical power	40
<b>Figure 39.</b> Complete circuit	42
<b>Figure 40.</b> Top side of PCB	43
<b>Figure 41.</b> Bottom side of PCB	43
<b>Figure 42.</b> Comparison of Matlab and Python execution time for common technical computing tasks in statistics, engineering calculations, and data visualization. Each point represents the time of a single test run in each language [16].	47
<b>Figure 43.</b> Startup	48
<b>Figure 44.</b> TCP/IP object definition and open connection	48
<b>Figure 45.</b> ITU channel selection	49
<b>Figure 46.</b> PCB board mounted	50
<b>Figure 47.</b> Hardware setup	51
<b>Figure 48.</b> ITU Channel 54 spectrum	51
<b>Figure 49.</b> ITU Channel 25 spectrum	52
<b>Figure 50.</b> ITU Channel 30 spectrum	52
<b>Figure 51.</b> ITU Channel 41 spectrum	52

## LIST OF TABLES

Table 1. NYW-30-009 ALTITUN GCSR laser aspects.	11
<b>Table 2.</b> Physical output current correspondence	44
<b>Table 3.</b> Input-output relationship	53
<b>Table 4.</b> Project budget	54

## **CHAPTER 1**

### **INTRODUCTION**

#### **1.1 PROJECT OVERVIEW**

The project was developed in the department of Signal Theory and Communications (TSC) at the Technical University of Catalonia (UPC), based on a proposed project by the supervisor Dr. José Antonio Lázaro.

The purpose of this project was to take advantage of the capabilities and easy programming of STEMLab Red Pitaya, an open source measurement and control tool that substitutes many expensive laboratory instruments for a low price embedded FPGA/DSP, so that we can control a tuneable laser. A tuneable laser is a laser whose wavelength of operation can be modified in a controlled manner. Tuneable lasers find applications in spectroscopy, photochemistry, medicine and optical communications [10]. Therefore, it would be of a high interest to gain an easy access to this tuneable laser by controlling it with high level programming.

#### **1.2 PROJECT GOALS**

The goals of the project were:

1. To know the characteristics of the laser and control current requirements.
2. To analyse the use of Red Pitaya to control four currents and monitor power and wavelength.
3. To design a PCB for the tuneable laser, also including a soft start.
4. To analyse the precision and stability of the circuit.

### 1.3 REQUIREMENTS AND SPECIFICATIONS

The requirements for the project are to provide:

1. A designed and implemented functional circuit
2. An experimentally characterization of the set of values for the four control currents required to tune the laser into the ITU (International Telecommunication Union) channels from 17 to 58 with the selected hardware.
3. A transparent input-output relationship code.

The specifications of the project are basically to implement a designed, programmed hardware and to provide laser operation so that any of the following ITU channels can be achieved.

## **CHAPTER 2**

### **STATE OF THE ART**

The objective of this section is to present an overview of the technology applied in this thesis. First, an introduction of semiconductor lasers will be given, latter on focusing on the GCSR lasers, because it is the one that has been used in this work. Second, the Red Pitaya tool, its capabilities and functions for this work will be described. Finally, the software for the PCB board design that has been employed will be mentioned.

### **2.1 SEMICONDUCTOR LASER**

The semiconductor laser, usually used as based element for optical transmitters, provides optical carriers by converting an electrical input signal into a monochromatic optical signal. Some transmitters directly modulate the output power of the laser or the frequency emission of the laser, or even the phase of the optical signal emitted by the laser by fast variations of some of the electrical currents that control the light emitted by the laser [11]. Alternatively, other optical transmitters modify the light properties by an external modulator [12]. Finally, the light carrying the information provided by the variations of the electrical currents is then launched it into the optical fiber serving as the communication channel. Semiconductor lasers present many advantages such as compact size, high efficiency, good reliability, wide wavelength range, and small emissive area, and for example, optical fibre communications developing would having impossible without the parallel research into efficient and compact semiconductor lasers [13].

#### **2.1.1 SEMICONDUCTOR LASER ARCHITECTURE**

The concept of semiconductor lasers is based on the emission and absorption of light due to the transition of atoms of the medium among the energy states in the semiconductor material.

Light can be emitted through spontaneous emission and stimulated emissions. Spontaneous emission occurs spontaneously and photons are emitted in random phases and directions, whereas the stimulated emission is initiated by an existing photon and the light is emitted in the same phase and direction as the original photon. When the current reaches a value, called the current threshold, the laser produces light output. The concept of laser threshold can be understood by noting that a certain fraction of photons generated by stimulated emission is lost because of the competitive phenomena of absorption by the cavity and it needs to be created continuously. If the optical gain is not large enough to compensate for the cavity losses, a net gain cannot be created. So, we need a minimum amount of gain for the laser operation. In the semiconductor laser, this optical gain is amplified by the optical feedback provided by the laser facets acting as partially reflective mirrors (Fig. 1).

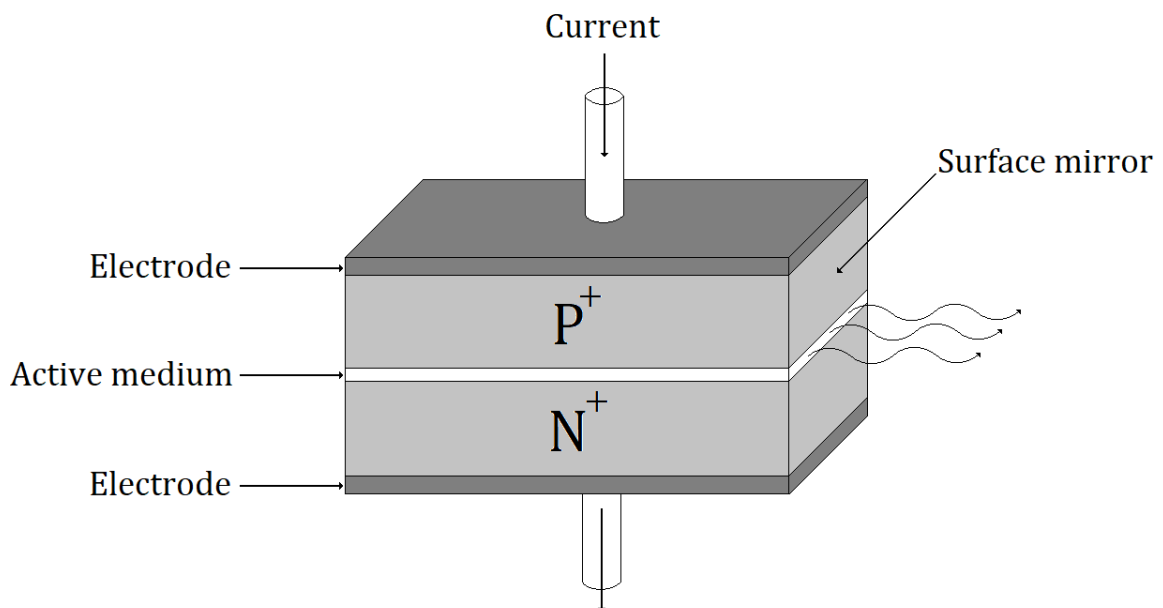


Figure 1. Fabry-Perot cavity laser

Because of partial reflections at the two surface mirrors, the transmitted light waves are added in phase for the resonant wavelengths of the cavity. All the wavelengths that satisfy this condition are called the longitudinal modes of that laser. As a result of in-phase addition, the amplitude of the transmitted wave is greatly increased for

these resonant wavelengths compared to other wavelengths. Because of a relatively small gain difference between neighbouring modes, such lasers oscillate in several longitudinal modes of the cavity leading to a broad spectral width (Fig. 2).

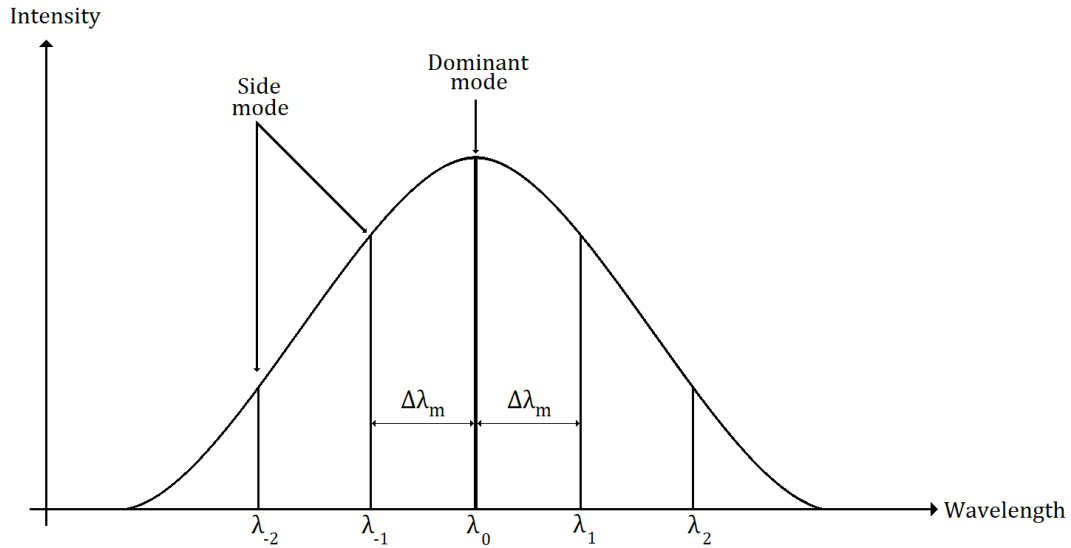


Figure 2. Wavelengths of the  $i$ -th longitudinal mode

Wavelengths of the  $i$ -th longitudinal mode satisfy the next condition:

$$\lambda_i = \frac{2Ln}{i} \quad (2.1)$$

where  $L$  is the length of the cavity and  $n$  the refractive index. The longitudinal mode spacing satisfies:

$$\Delta\lambda_m = \frac{\lambda_0^2}{2nL} \quad (2.2)$$

Typical values for longitudinal mode spacing are:  $\Delta\lambda_m = 0.3 - 1$  nm.

## 2.2 TUNEABLE LASER

A tuneable laser is a laser in which the output wavelength can be adjusted. In some cases, particularly wide tuning range is desired, i.e., a wide range of accessible wavelengths, whereas in other cases it is sufficient that the laser wavelength can be tuned to a certain value. Some single-frequency lasers can be continuously tuned over a certain range, whereas others can access only discrete wavelengths or at least exhibit mode hops when being tuned over a larger range.

Tuneable semiconductor lasers are very important for optical communications. They have already been used in some networks for several years, starting with devices with a small tuning range, but moving towards full-band tuning [14]. Tuneable lasers will, of course, have to meet the same specifications as fixed-wavelength lasers; this includes optical power, wavelength accuracy, relative intensity noise (RIN), side-mode suppression ratio (SMSR), etc. An important additional requirement is that it has to be optically isolated from the network during wavelength switching in order to avoid polluting the network with light emitted during the switching process.

There are many types of semiconductor tuneable laser as described in [15]. Fig. 3 gives a schematic of a generic tuneable laser. In most practical embodiments, the filter, mirror and phase-shifting elements are combined in some way to create a unique physical structure for different kinds of tuneable lasers.

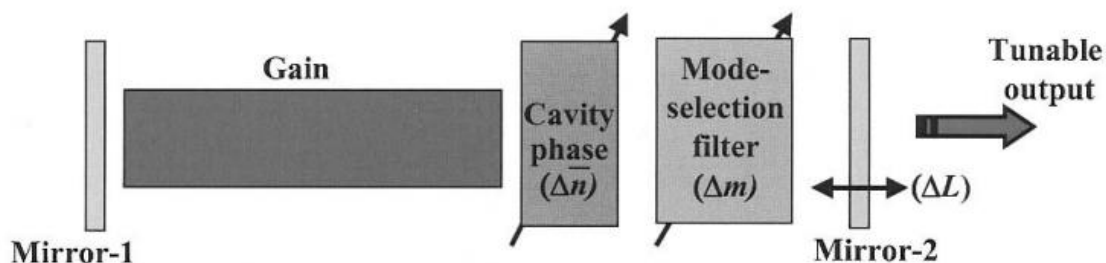


Figure 3. Schematic of a generic tuneable laser [15].



Fig. 3 can be used to see how a tunable semiconductor laser evolves from the most basic Fabry-Perot laser, which has just the gain and the two simple mirror elements, to a “single-frequency” laser, which adds the mode-selection filter, to a “tunable single-frequency” laser, which adds possible adjustment of the mirror position and the center frequency of the mode-selection filter, as well as adding an adjustable cavity phase element.

The most common single-frequency laser is the distributed-feedback (DFB) laser, as shown in Fig. 4(a), in which an index grating is formed near the optical waveguide to provide a continuous reflection that gives both the mirror functionality as well as the mode selection filter. The vertical-cavity single-frequency laser (VCSEL), as illustrated in Fig. 4(b), is also a single-frequency laser, but in this case the cavity is vertical and the grating mirrors sandwich the gain region.

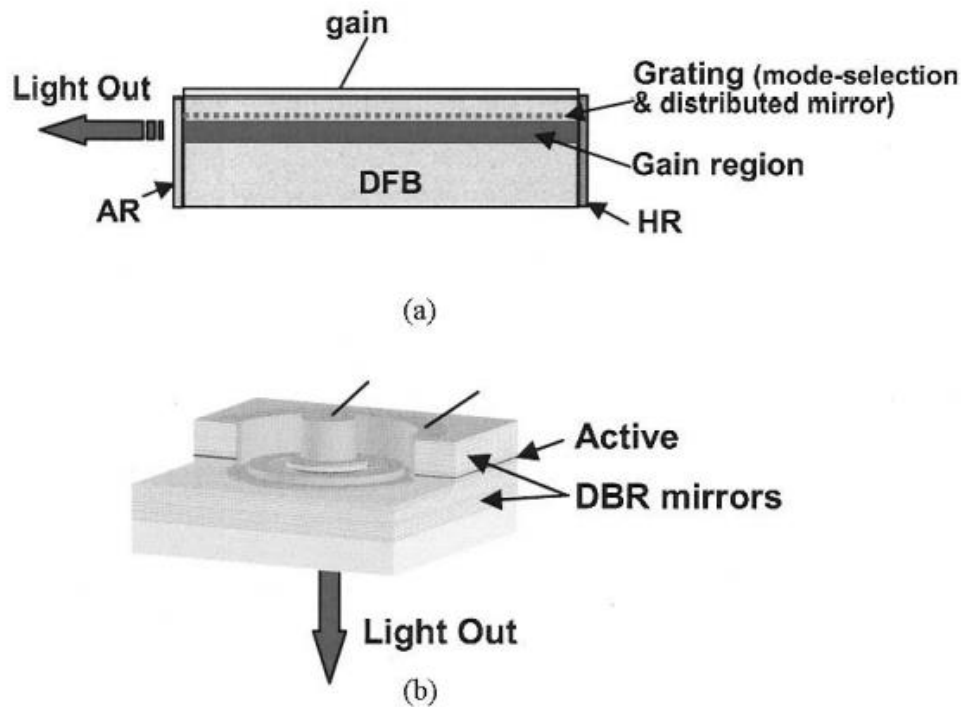


Figure 4. Examples of single-frequency lasers (not tunable): (a) DFB laser and (b) VCSEL [15].

Some examples of tunable single-frequency lasers are shown in Fig 5. Fig. 5(a) shows a selectable array of DFB lasers that are combined in a multimode interference coupler. The DFBs are excited one at a time and each is manufactured with a slightly different grating pitch to offset their output wavelengths by about 3 or 4 nm.

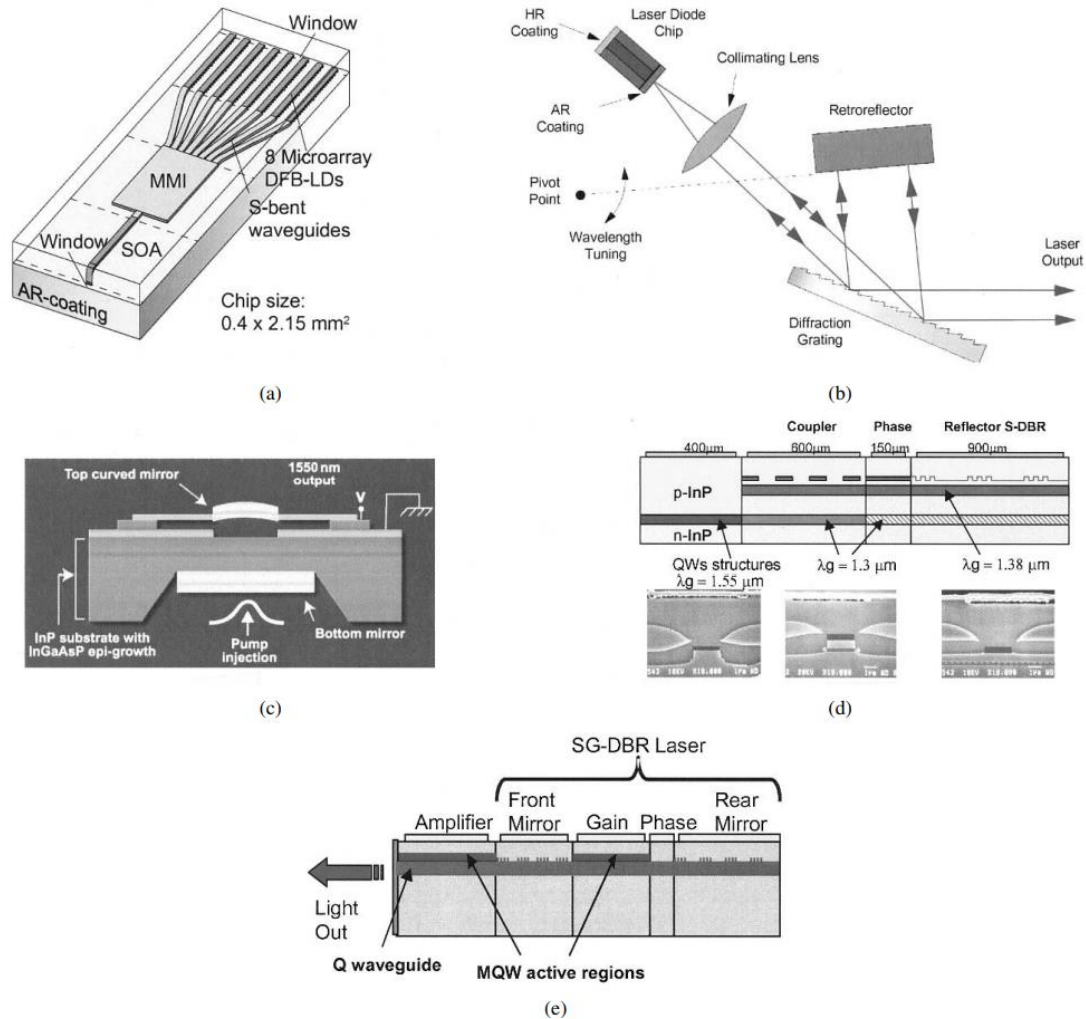


Figure 5. Examples of widely-tunable laser types: (a) selectable DFB array, (b) external cavity, (c) MEMs/VCSEL, (d) Grating-Coupled Sampled-Reflector (GCSR) and (e) sampled-grating DBR (SG-DBR) with integrated SOA [15].

Fig. 5(b) is an example of an external-cavity laser. A “gain block” is coupled to external mode-selection filtering and tuning elements via bulk optical elements. Fig. 5(c) shows a tunable VCSEL that is created by mounting one mirror on a flexible arm and using an electrostatic force to translate it up and down.

Fig. 5(d) and (e) show monolithic widely-tunable semiconductor laser approaches that employ electronic tuning of the index in a single cavity to provide for full C- or L-band wavelength coverage. Both are variations on older DBR laser approaches, but both employ concepts to tune the relative wavelength by up to an order of magnitude more than the index of any section can be tuned. In the SGDBR of Fig. 5(e), the wider tuning range filter is provided by the product of the two differently spaced and independently tuned reflection combs of the SGDBRs at each end of the cavity. In the case of Fig. 5(d), the grating-coupled sampled-reflector (GCSR) laser is accomplished by using a property of a grating-assisted co-directional which has a tuning proportional to the index tuning relative to the difference in index between two coupled waveguides,  $\Delta n/(n_1 - n_2)$ , rather than  $\Delta n/n_1$  as in most other filters.

For the project, we will be focusing on GCSR lasers as it is on the tuneable semiconductor laser providing a wider range of tuneability [15].

### 2.3 GRATING ASSISTED COUPLER WITH SAMPLED REAR-REFLECTOR (GCSR) LASER

A GCSR laser consists of four sections: gain block, phase module, coupler and reflector grating.

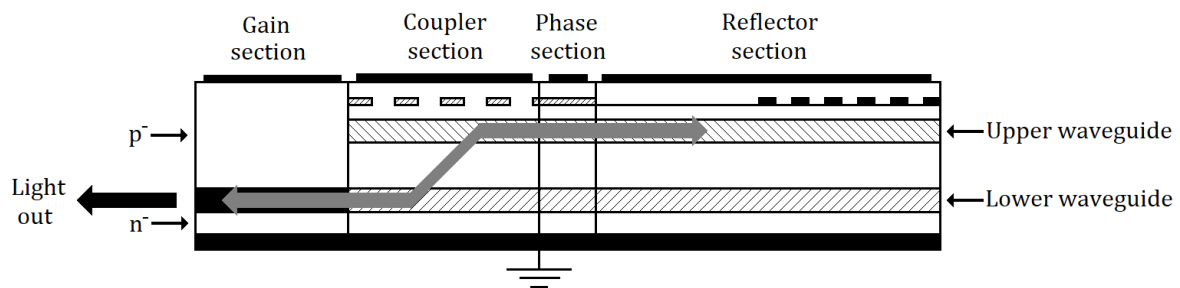


Figure 6. Detail of the four sections of a GCSR laser with the wavelength path [1].

The coupler section acts as a coarse tuner, transferring power vertically between the two waveguides (Fig. 3), one that runs forward to the gain block, and another one, above it, that runs backward into the phase and reflector sections. Increasing coupler current the filter shifts to lower  $\lambda$ , this is a kind of coarse tuning. As reflector current

increases, the comb filter shifts to shorter wavelengths. Fine tuning is done by current injection on the phase section, which tunes all cavity modes simultaneously. The four sections make fine and stable wavelength tuning possible with a tuning range of about 40 nm, covering the whole C-band required for optical communications and allowing efficient use of spectral bandwidth.

## 2.4 NYW 30-009 GCSR LASER

The NYW 30-009 GCSR laser is a continuous wave (CW) widely tuneable laser module whose output signal can be tuned 4 THz (~32 nm) from 192.05 to 196 THz.



*Figure 7. NYW 30-009 ALTITUN GCSR laser in butterfly package*

### Pin Number and Function

Pin function	Pin function
1. TE cooler anode (+)	8. Monitor photodiode anode (+)
2. Thermistor	9. NC
3. Thermistor	10. Chip and package ground
4. Gain current (+)	11. Phase current (+)
5. Package ground	12. Coupler current (+)
6. Reflector current (+)	13. NC
7. Monitor photodiode cathode (-)	14. TE cooler cathode (-)

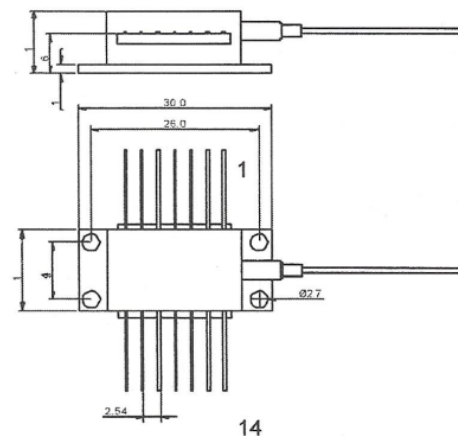


*Figure 8. NYW 30-009 ALTITUN GCSR pin configuration*

	SYMBOL	MIN	TYP	MAX	UNIT
Operating currents					
Gain section	$I_G$		100	150	mA
Coupler section	$I_C$	0		60	mA
Reflector section	$I_R$	0		50	mA
Phase section	$I_P$	0		10	mA
Accuracy required to maintain frequency within $\pm 5\text{GHz}$ and $\text{SMSR} > 23\text{dB}$					
Gain section	$\Delta I_G$			$\pm 10$	mA
Coupler section	$\Delta I_C$			$\pm 0.03$	mA
Reflector section	$\Delta I_R$			$\pm 0.01$	mA
Phase section	$\Delta I_P$			$\pm 0.1$	mA
Optical characteristics					
Output power	$P_{OUT}$	-3	0		dBm
Side mode suppression ratio	$\text{SMSR}$	30	35		dB
Linewidth	$\Delta\nu$		25		MHz
Polarization extinction ratio	$\text{PER}$	17	20		dB
Tuning range	192.05 – 196.00 THz				
TEC and Thermistor Characteristics					
Current	$I_{TEC}$			1.2	A
Voltage	$V_{TEC}$			3.4	V
Thermistor resistance, nominal (25°C)			10		kΩ
Thermistor equation coefficients	$A = 1.129 \cdot 10^{-3}, B = 2.341 \cdot 10^{-4}, C = 8.775 \cdot 10^{-8}$				

Table 1. NYW 30-009 ALTITUN GCSR laser aspects

The emission at a tuned wavelength is achieved by supplying the appropriate combination of tuning currents to the four sections of the laser. It has two inputs per electrode, one for injecting the tuning bias current for continuous wave lasing and another with a 50-ohm resistor matched, so this board also allows direct modulation on each of the laser electrodes.

In order to maintain constant optical output power during continuous wavelength lasing, it is desirable to make the injected laser current independent of temperature. Therefore, the laser bias is driven with a high impedance current source. The laser is also fitted with a thermo-electric (TE) cooler to maintain constant laser chip temperature so that optical power remains constant at constant current.

### 2.4.1 GAIN SECTION

For the laser to work in stimulated emission, the current at gain section has to be well above the lasing threshold. For the GCSR, threshold is nearly 20 mA as it can be appreciated in Fig. 5.

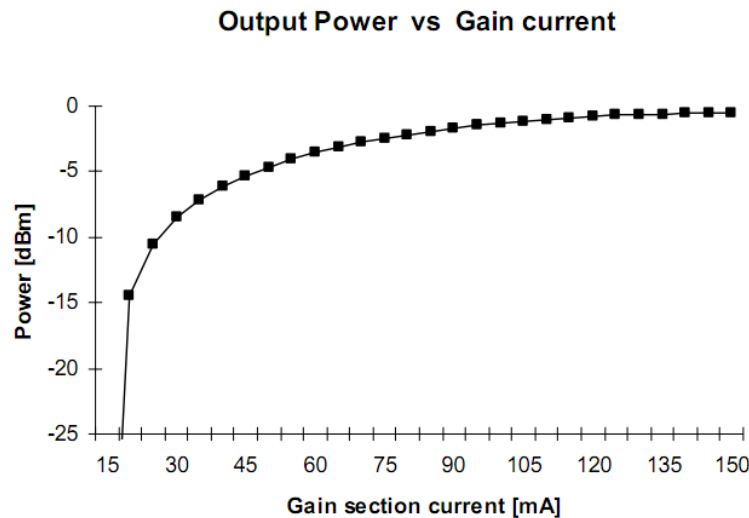


*Figure 9. Power output versus gain current for a fixed coupler current of 10 mA, reflector current of 12.5 mA and a phase current of 0.3 mA at  $T=25^{\circ}\text{C}$  [1].*

As it can be seen, the typical constant current for gain section is around 100 mA, but higher output power could be achieved by applying a higher current (up to 150 mA).

## 2.4.2 COUPLER SECTION

Coupler section is used for coarse tuning. The slope of the wavelength variation is of 3.5 nm/mA, whilst into the same mode the variation is only of about  $1e^{-10}$  nm/mA.

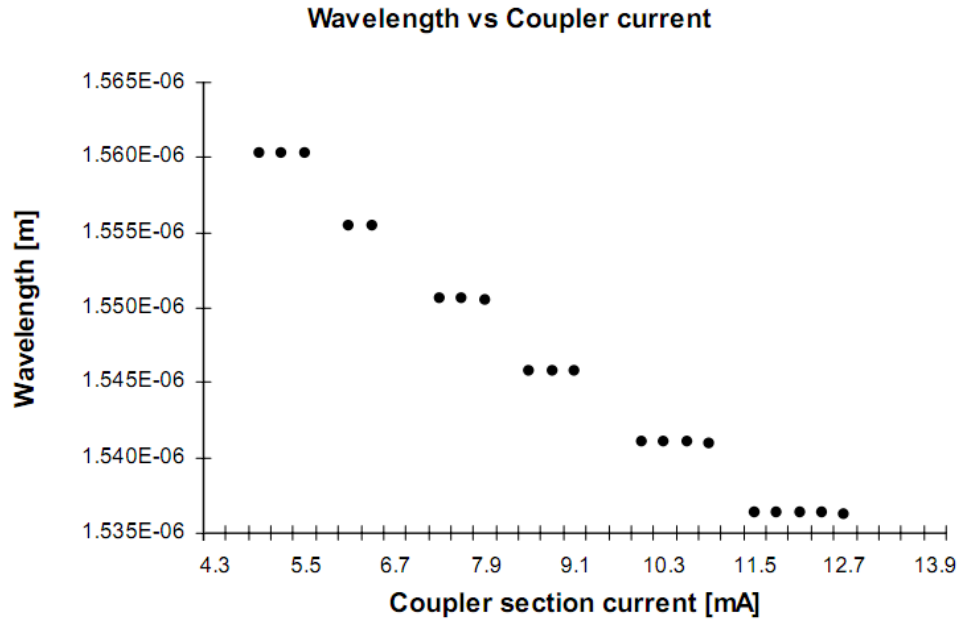


Figure 10. Wavelength versus coupler section current for a fixed reflector current of 3 mA and phase current of 1 mA at  $T=25^{\circ}\text{C}$  [1].

## 2.4.3 REFLECTOR SECTION

Reflector section contains a Bragg grating. A Bragg grating is a type of reflector that reflects particular wavelengths of light and transmits all others. Therefore, it can be used as an inline optical filter to block certain wavelengths, or as a wavelength-specific reflector.

As reflector current rises, sampled Bragg reflector selects lower order laser cavity modes; hence, mode jumps of  $\sim 0.27$  nm can be observed in Fig. 7. Reflector section is used for fine tuning.

Wavelength vs Reflector section current

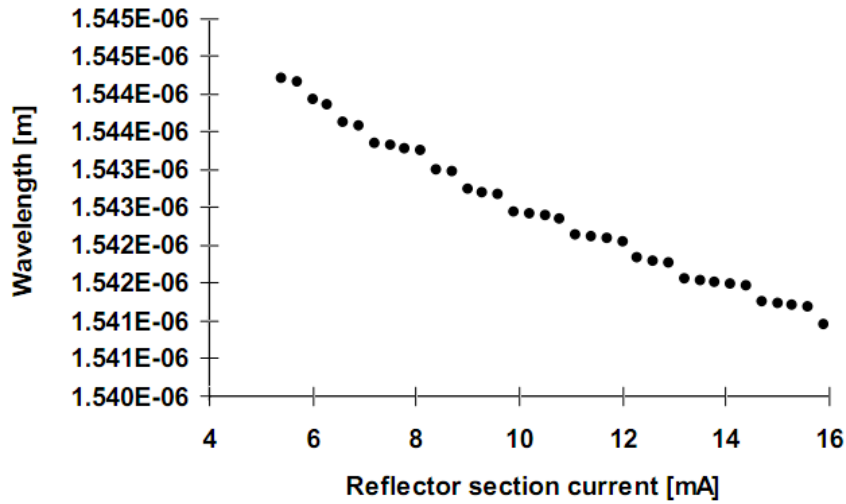


Figure 11. Reflector section current-wavelength characteristics for a fixed coupler current of 9.7 mA and phase current of 1 mA at  $T=25^{\circ}\text{C}$  [1].

#### 2.4.4 PHASE SECTION

Phase section tunes all optical cavities simultaneously. An optical cavity is a pair of mirrors that forms a standing wave cavity resonator for light waves. Optical cavities are a major component of lasers, surrounding the gain medium and providing feedback of the laser light.

Wavelength vs Phase current

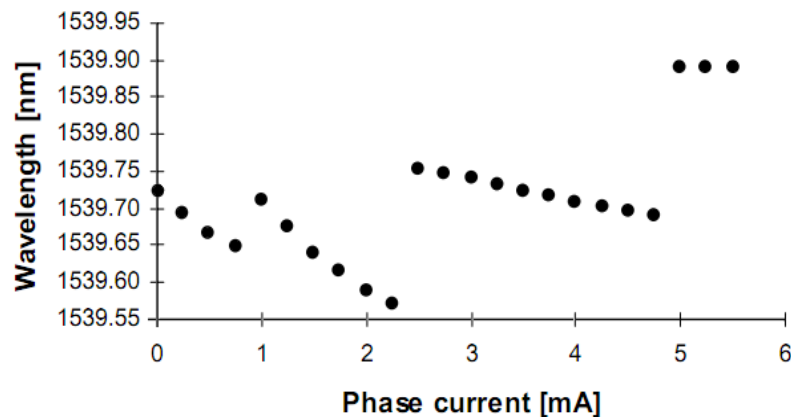


Figure 12. Phase section current-wavelength characteristics for a fixed coupler current of 11 mA and reflector current of 5 mA at  $T=25^{\circ}\text{C}$  [1].



For gain section, current range is from 20 mA to 150 mA. The wavelength variation, in comparison with the current effect on the tuning sections, is negligible. Useful ranges for coupler and reflector sections are from 4 to 34 mA, but this depends on the device unit. Even though the phase current range available is from 0 to 8 mA, the useful range, having continuous phase zones, is from 0 to 5 mA.

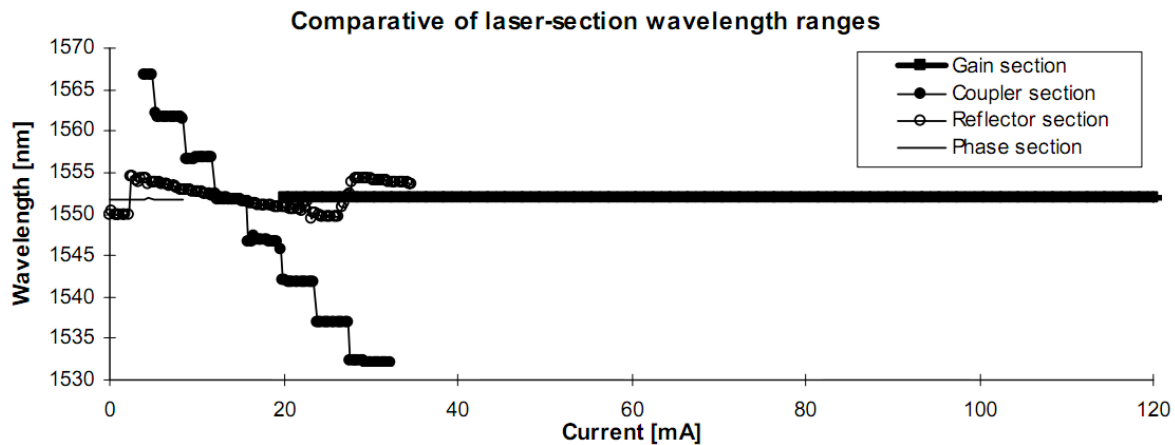


Figure 13. Wavelength and current ranges for each GCSR section at  $T=25^{\circ}\text{C}$  [1].

Small current injection on gain section does not produce wavelength change. For tuning sections, phase section presents the largest continuous range of wavelength change.

## 2.5 STEMLab Red Pitaya

Red Pitaya is a closed-source hardware, open-source software project intended to be an alternative for many expensive laboratory measurement and control instruments. This powerful tool is at the heart of a revolutionary Red Pitaya ecosystem, which facilitates discovering, experiencing, learning, developing and sharing a variety of applications.

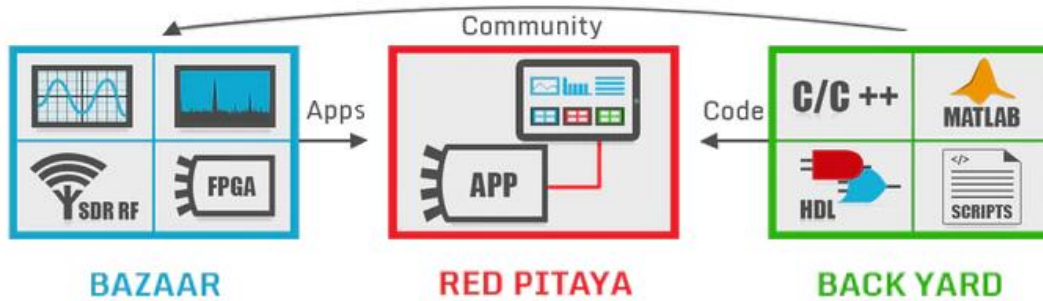


Figure 14. Red Pitaya Ecosystem

The Red Pitaya ecosystem consists of:

- Red Pitaya, a high-performance tool at a surprising price tag.
- Bazaar, a free of charge marketplace where open source applications are available within a single click for immediate experience and use. Initial set includes:
  - Oscilloscope
  - Spectrum analyser
  - Arbitrary signal generator
  - Frequency response analyser
  - PID controller

which can all be accessed by any web browser from tablet or laptop computer.

- Backyard, an organized repository containing the corresponding open source code and tools necessary for developing applications.
- Spark Center, is a place to share and contribute new ideas, post sketches or proposals to create inputs for new Red Pitaya applications and hardware extension modules.

Red Pitaya is a great springboard for electronics enthusiasts, because it offers great user interface and can be easily reconfigured for any kind of interaction with the outside world by simply modifying the available applications.

The learning process is simplified by Red Pitaya Backyard containing all the application's source code. Programming can be started by applying incremental changes to the code and publishing the work in Bazaar and easily get in touch with a wide range of technologies and knowledge. It is also appropriate for PhD or other research projects, because it is a very suitable solution for detecting and analysing fast phenomena, as well as generating or simulating complex signals.

Red Pitaya applications include open source code on all levels of programming (HDL, C/C++ application, Python, Matlab, WEB user interface) and therefore they accelerate development and shorten time.

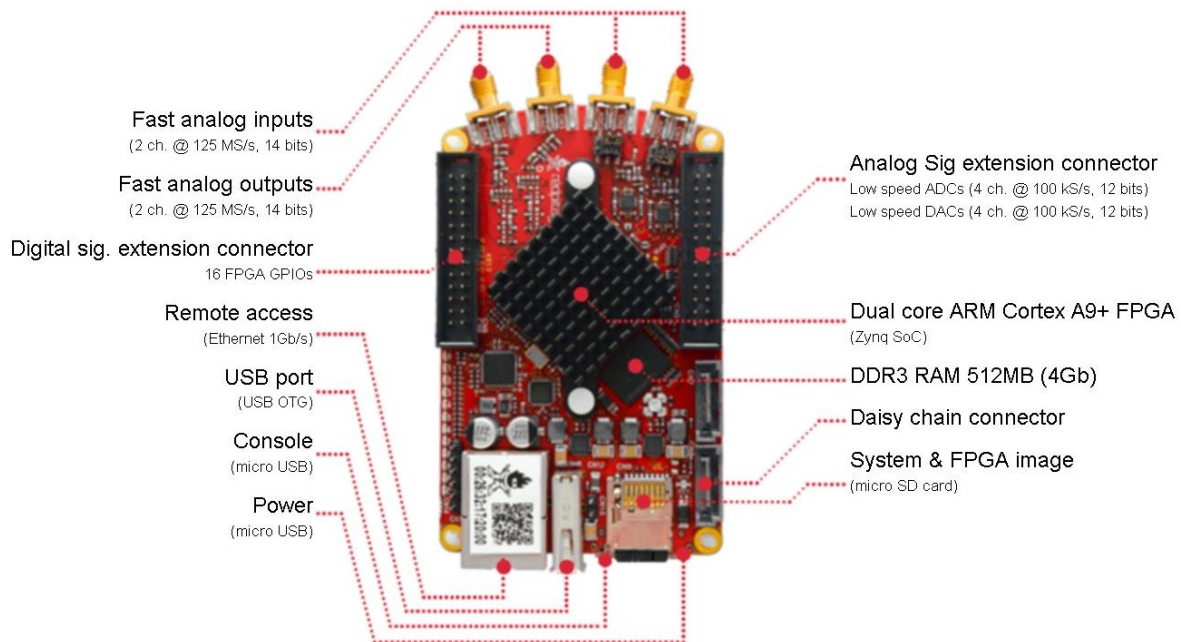


Figure 15. Red Pitaya hardware overview

Red Pitaya can be controlled remotely over LAN or wireless interface using Matlab, Labview, Scilab or Python via Red Pitaya SCPI (Standard Commands for Programmable Instrumentation) list of commands. SCPI interface/environment is commonly used to control T&M (time and materials) instruments for development, research or test automation purposes. SCPI uses a set of SCPI commands that are recognized by the instruments to enable specific actions to be taken, for example,

acquiring data from fast analog inputs, generating signals, controlling other periphery of the Red Pitaya STEMLab platform, among others. The SCPI commands are very useful when complex signal analysis is required and where SW environment such as Matlab provides powerful data analysis tools and SCPI commands simple access to raw data acquired on the board.

In summary, Red Pitaya allows to:

- Quickly write control routines and programs using Matlab, Labview, Scilab or Python.
- Use powerful data analysis tools of Matlab, Labview, Scilab or Python to analyse raw signals acquired by Red Pitaya.
- Write testing scripts and routines.
- Incorporate your STEMLab and Labview into testing and production lines.
- Take quick measurements directly with your PC.

## CHAPTER 3

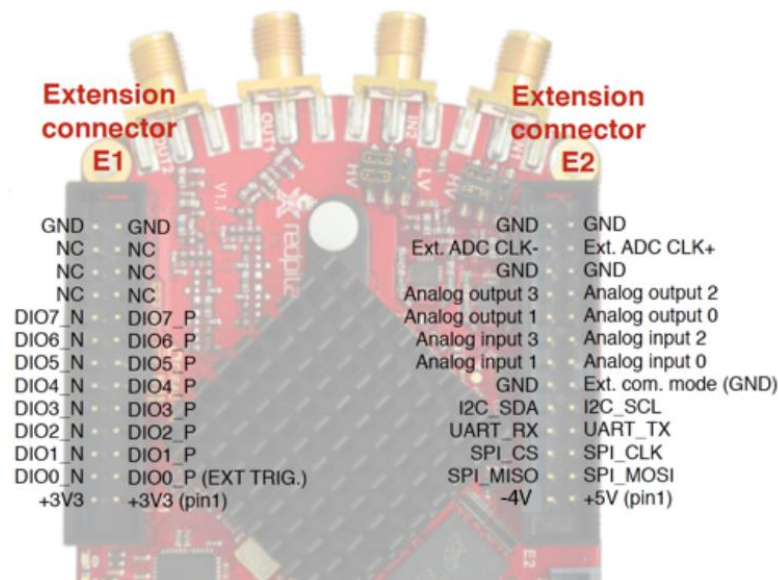
### PROJECT DEVELOPMENT

#### 3.1 Red Pitaya TESTING

In order to check the suitability of this tool for controlling voltages, the first step was to run the demo codes provided by the manufacturer and to analyse the behavior of the tool. For that, the Red Pitaya was configured. In Fig. 12 the characteristics of the extension connector can be seen and where the 16 I/O pins are located.

Extension connector	
	STEMLAB 125-14
Digital IOs	16
Analog inputs	4
Analog inputs voltage range	0-3,5V
Sample rate	100kS/s
Resolution	12bit
Analog outputs	4
Analog outputs voltage range	0-1,8V
Communication interfaces	I2C, SPI, UART
Available voltages	+5V,+3,3V,-4V
external ADC clock	yes

(a)



(b)

Figure 16. (a) Extension connector characteristics and (b) I/O pins location.

The Red Pitaya OS was installed in a SD card of at least 8GB. To have a wireless communication, the Red Pitaya and the computer had to be connected to the same router using ethernet cable. Then, *rp-XXXXXX.local* was typed in the URL, where the “XXXXXX” were the last 6 digits of the MAC address of the Red Pitaya. After that, the Red Pitaya STEMLab main page appeared, as shown below.

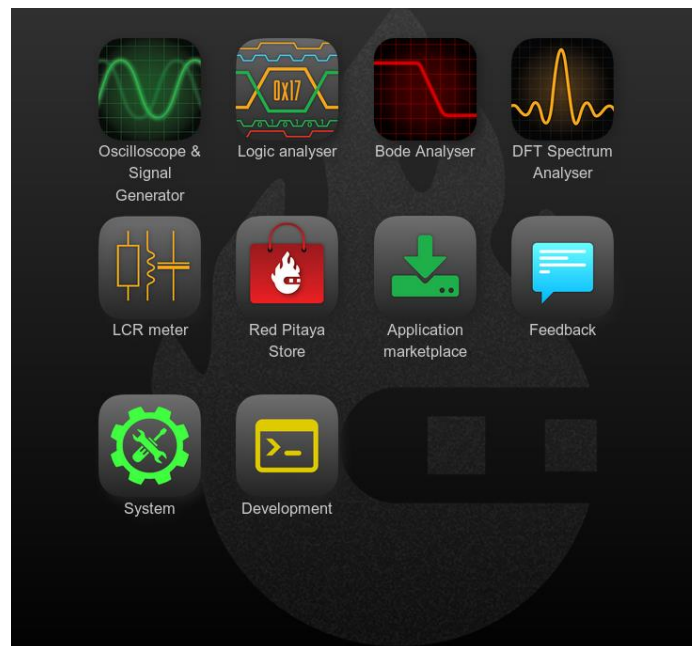


*Figure 17. STEMLab main page*

Next, the instructions of the Red Pitaya manual were followed. The instructions were:

- 1) Start your STEMLab web user interface.
- 2) Open Network Manager application
- 3) Insert Wi-Fi dongle in the USB plug on the STEMLab board.



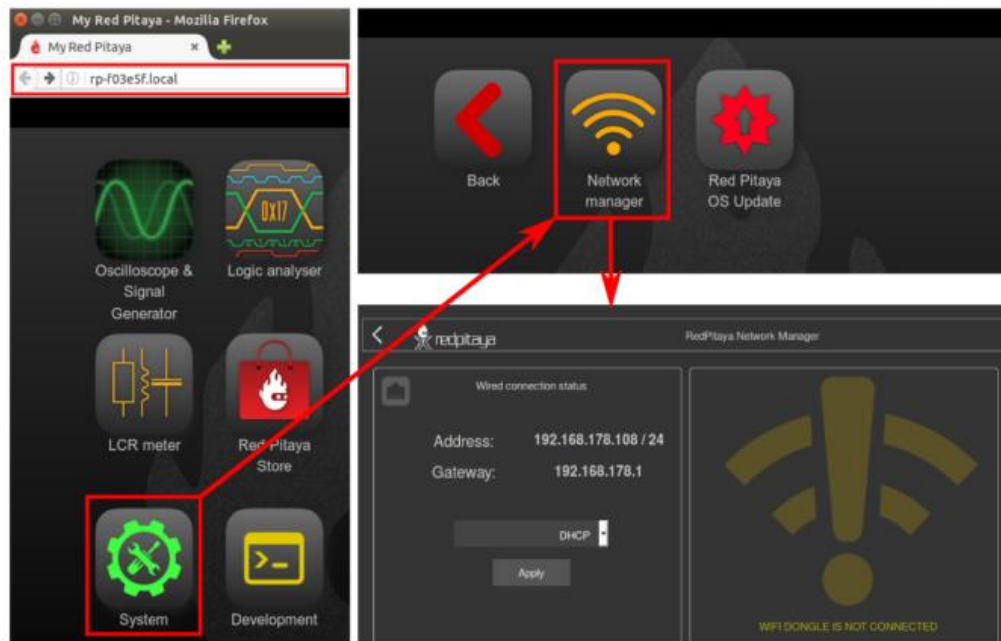


Figure 18. STEMLab network manager

- 4) When the USB Wi-Fi dongle is plugged in, the system will recognize it and enabled additional settings.
- 5) Select Client Mode, Desired Wi-Fi network. Insert password and click Connect.
- 6) When your STEMLab board is connected, the IP address will be shown on the user interface. This IP address is only for Wi-Fi connection. The connection can be checked by inputting a Wi-Fi IP address in the web browser URL field.

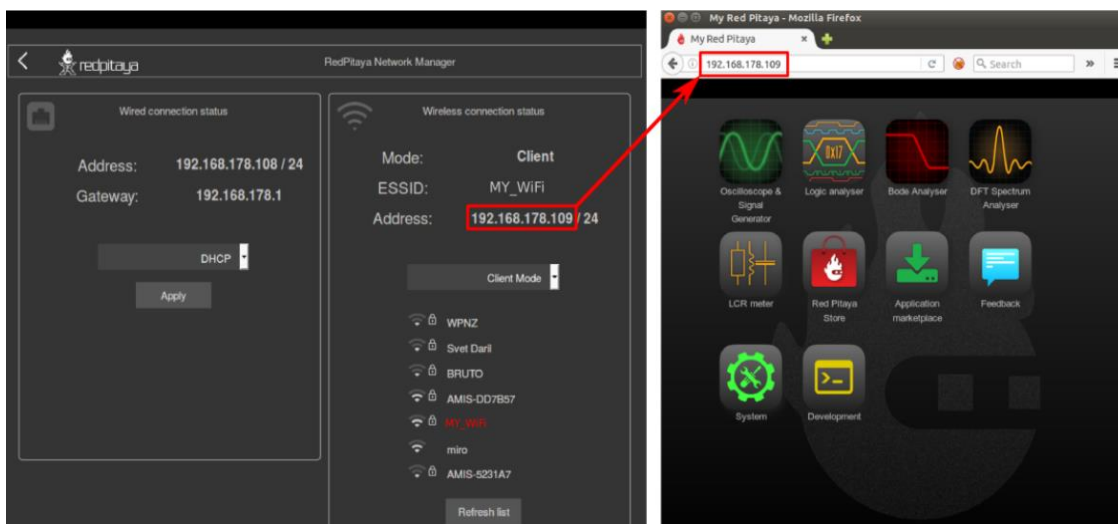


Figure 19. Wireless connection established

After establishing wireless connection, Matlab with Red Pitaya had to be connected. For that, the steps written in the Red Pitaya manual were followed:

- 1) Go to your STEMLab main page and select Development, then SCPI server.
- 2) Start SCPI server by selecting RUN button. Please notice the IP of your STEMLab board as it will be needed to connect your board.

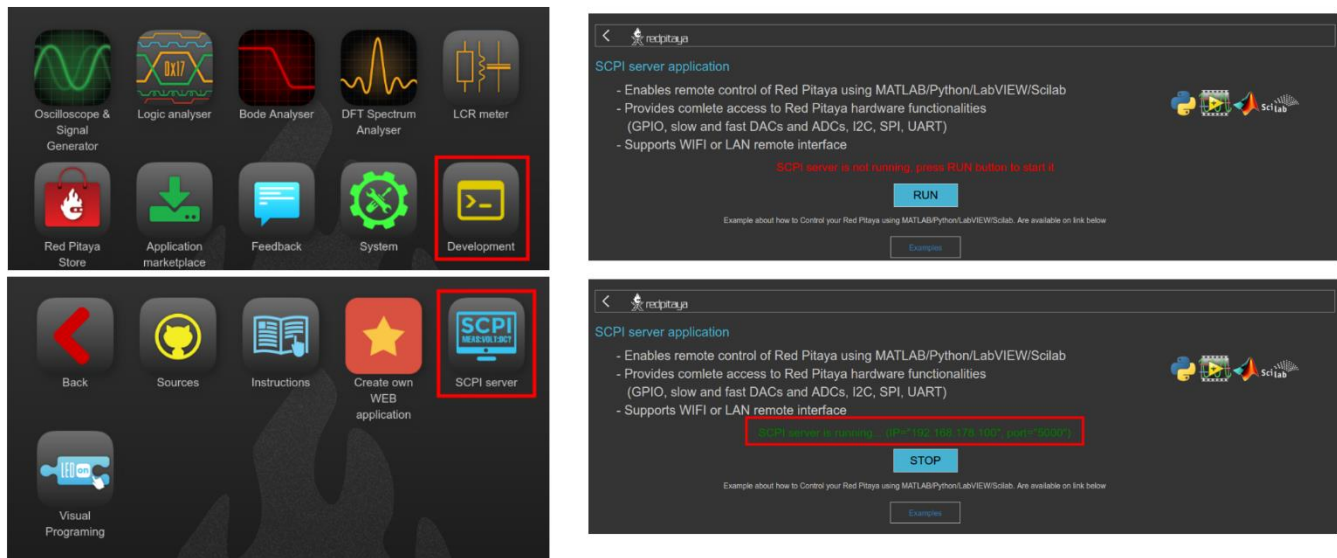


Figure 20. SCPI connection

Once the connection between Matlab and Red Pitaya was reached, the analog output pins were tested. Changing the code, the voltage wanted to be delivered in each of the analog output pins was selected, as long as it is within the range of 0 to 1.8 volts. To read the voltage, a mutimeter was used.



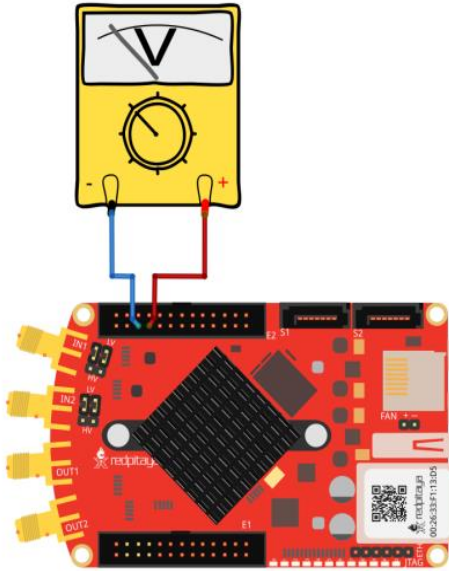


Figure 21. Testing of the analog output pins

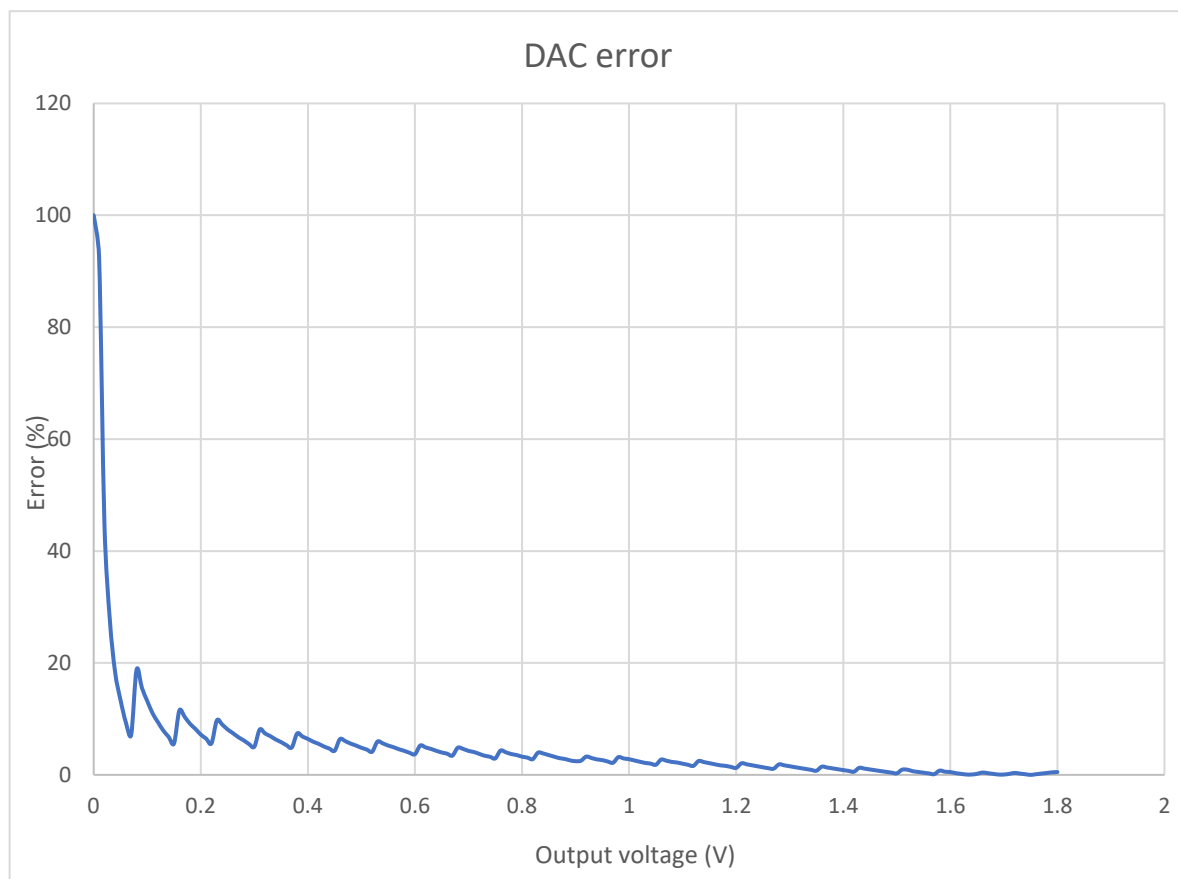


Figure 22. Analog output error.

As it can be seen, the error minimized as the output voltage increased. The resolution specification for the DAC and ADC pins are 12 bits. Therefore, a step size of 0.493mV was expected. Even though, it was found that the minimum increase of the voltage is by tens of millivolts. By increasing it in millivolt unit, the output voltage didn't show any change. The error is the same in the four analog outputs.

Later, the DAC input error was checked, to know if a good reading of the output voltage for control would be obtained. An output pin was connected to an input pin of the DAC.

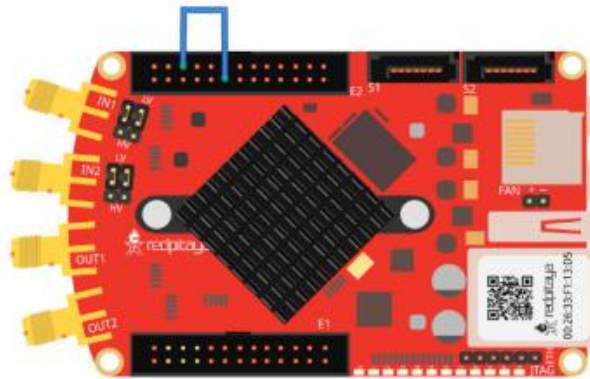


Figure 23. Testing of the analog input pins

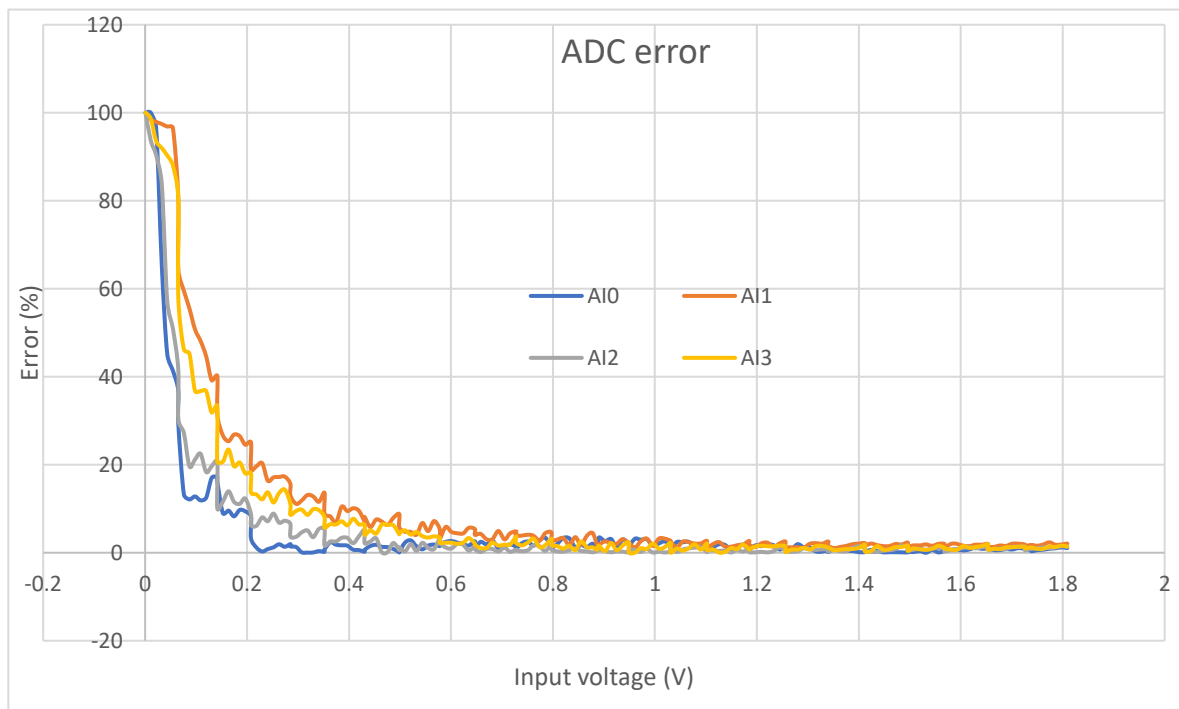


Figure 24. ADC error

As it can be observed, the behaviour of the ADC was similar to the DAC but with a lot of noise, something undesired for the control of the voltages because the error could not be compensated.

## **3.2 HARDWARE DESIGN**

### **3.2.1 HARDWARE REQUIREMENTS**

The GCSR laser is a sensitive element, so the system to be designed needs to have the resources for its protection, such as supply filtering, soft start, current limiters, temperature controller and optical measurement.

This means that it is necessary to design four stages:

- 1) Voltage regulator with soft start
- 2) Limited current sources
- 3) Temperature controller
- 4) Optical measurement

The function and design of each section have been described in the following sections.

#### **3.2.1.1 VOLTAGE REGULATOR WITH SOFT START**

Soft start is the gradual turning on of an electronic power supply to avoid stressing the components by the sudden current or voltage surges associated with the initial charging of capacitors and transformers. The soft start function in a power supply circuit minimizes large start-up currents from flowing when the input power is first applied. As power is first applied to a circuit, the capacitors must be charged from zero to their final values, while the inductors and transformers need to have their flux stabilized. Likewise, the integrated circuits and other active components must change from the inactive states to active states.

There are various ways of implementing the soft start either using discrete components or integrated circuits. The choice depends on power rating of the

supply, the circuit design and the desired soft start period which varies from one design to another.

In the Red Pitaya extension connector E2, power supplies are available. The problem with them is that they have current limitations, 500 mA for +5V and +3.3V, 50 mA for -3.3V supply. Using these power supplies with their low current limitations could be risky for the Red Pitaya as well as for the designed hardware. Also, they don't have soft start. Therefore, the power supply with soft start was designed.

The energy that this design needs will be provided by a power source that delivers  $\pm 12V$ . But this value goes beyond what is needed, which is from  $\pm 2V$  to  $\pm 5V$ . So, a positive and negative voltage regulator had to be implemented to decrease the value of the power supply to the desired one. Fig. 12 shows the implemented schematic:

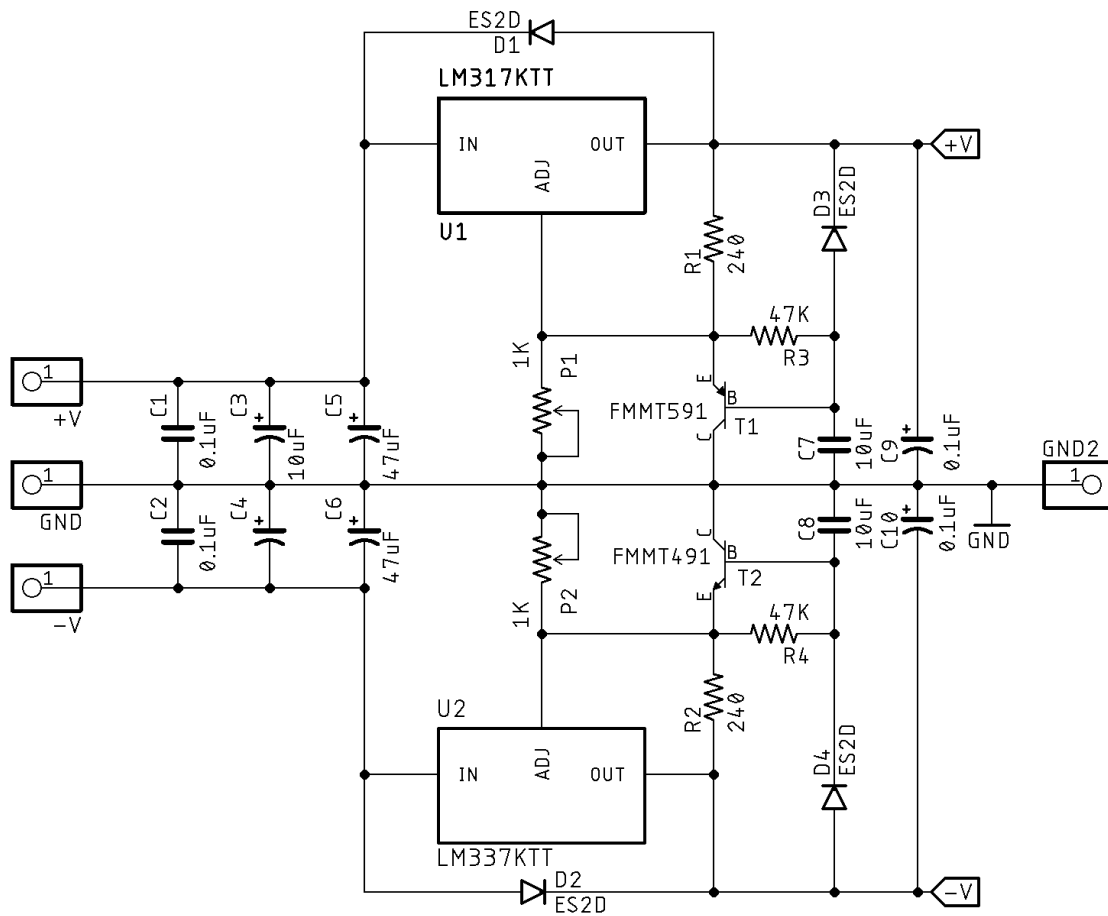


Figure 25. Positive and negative voltage regulator with soft start schematic.

The upper area is the positive voltage block and the lower area is the negative voltage block. Each of these blocks are composed of filtering, protections, voltage regulator and soft start.

Filtering stage is done by the use of capacitors C1, C2, C3, C4, C5 and C6, which dampen the connection between the power source and the circuit because it involves a sudden change in voltage. Protections are done by diodes D1, D2, D3 and D4. They protect the circuit against inverse currents that may occur in the on and off transients due to the charge and discharge of capacitors.

Voltage regulators, LM317 for positive voltage and LM337 for negative voltage, were used. They are capable of supply more than 1.5A over an output voltage range of 1.25V to 37V. They include current limiting, thermal overload protection, and safe operating area protection. Both of them have the same configuration.

Voltage regulators are configured by a resistance network to establish output voltage. The expression given by the manufacturer that calculates the output voltage desired is:

$$V_O = V_{ref} \left( 1 + \frac{R_{P1}}{R_1} \right) + I_{ADJ} \cdot R_{P1} \quad (1)$$

where  $V_O$  is the output voltage of the regulators and  $V_{ref}$  is the internal reference voltage that the regulator possesses and has a value of 1.25V. Current  $I_{ADJ}$  is negligible because it has a low value of 50μA and doesn't make any significant change in the output voltage value.

If we want an output voltage of 5V, we can find the values for resistances  $R_1$  and  $R_{P1}$  with the expression (1):

$$5V = 1.25V \left( 1 + \frac{R_{P1}}{R_1} \right) \quad (1.1)$$

$$\frac{R_{P1}}{R_1} = 3 \quad (1.2)$$

Expression (1.2) defines the ratio that  $R_1$  and  $R_{P1}$  have to follow so the output voltage of the regulator is 5V. For  $R_1$ , 240 $\Omega$  it was chosen and  $R_{P1}$  was determined with a potentiometer of 1K $\Omega$ , so an easy adjustment could be obtained. The output voltages for each regulator were:

$$V_+ = 1.25V \left( 1 + \frac{R_{P1}}{R_1} \right) \quad (1.3)$$

$$V_- = -1.25V \left( 1 + \frac{R_{P2}}{R_2} \right) \quad (1.4)$$

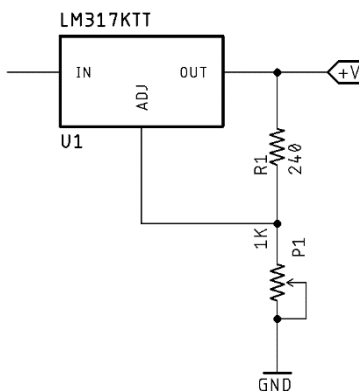


Figure 26. Voltage regulator.

Soft start consists of a RC network ( $R_3$  with  $C_7$  and  $R_4$  with  $C_8$ ), a bipolar transistor (FMMT491 and FMMT591) and a protection diode ( $D_3$  and  $D_4$ ). The main objective is to behave as a low pass filter by not passing the transients that come from the input. The output voltage will increase slowly in order to not affect the circuit with sudden variations.

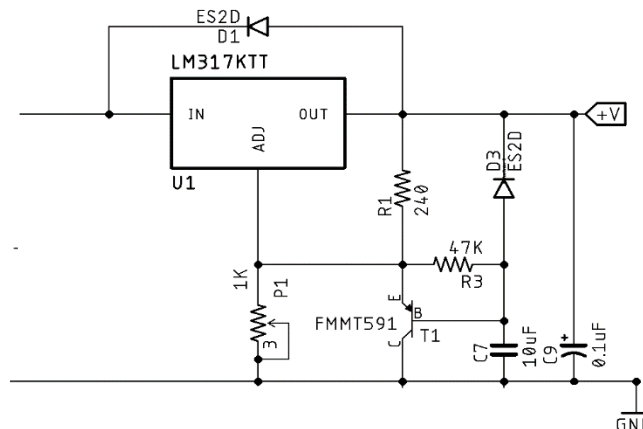


Figure 27. Voltage regulator with soft start.

The study of this stage supposes that the transistor is working in active mode and the capacitor is totally discharged. When the system was connected, two currents charge the capacitor  $C_7$ . One is the current that goes through the resistor  $R_3$  and the other one is the current coming from the base of the transistor.

$$I_{CHARGE} = I_R + I_B \quad (2)$$

$$I_R = \frac{V_{BE}}{R_3} = \frac{0.7V}{R_3} \quad (2.1)$$

$$I_B = \frac{I_C}{h_{fe}} = \frac{I_C}{460} \quad (2.2)$$

In the charging capacitor stage, these two currents could be approximated as constants. Base current of the transistor decreased when the potential difference in the capacitor was increased. The maximum voltage that the emitter of the transistor would be:

$$V_{E_{max}} = V_O - V_{ref} = 5V - 1.25V = 3.75V \quad (2.3)$$

Taking into account all of the above, the next step was to set the soft start time, and for that it was necessary to know the charging capacitor expressions:

$$Q = C \cdot V = I_{CHARGE} \cdot t \rightarrow t = \frac{C \cdot V}{I_{CHARGE}} \quad (2.4)$$

A soft start time of one second was set. The value of the capacitor to  $10\mu F$  was fixed. Therefore, the charge current was:

$$I_{CHARGE} = \frac{10\mu F \cdot 3V}{1s} = 30\mu A \quad (2.5)$$

And substituting this value in expression (2):

$$I_{CHARGE} = I_R + I_B = \frac{0.7V}{R_3} + \frac{I_C}{460} = 30\mu A \quad (2.6)$$

Current collector is the one that comes from the resistance  $R_1$  of the voltage regulator:

$$I_C = \frac{V_{ref}}{R_1} = \frac{1.25V}{240\Omega} = 5.2mA \quad (2.7)$$

Finally, clearing  $R_3$  from equation (2.6), its value was found:

$$R_3 = \frac{V_{BE}}{I_{CHARGE} - \frac{I_C}{h_{fe}}} = \frac{0.7V}{30\mu A - \frac{5.2mA}{460}} = 37.44K\Omega \quad (2.8)$$

A commercial resistance value was looked for and  $R_3$  to 47K $\Omega$  was fixed.

### 3.2.1.2 CURRENT SOURCES

As it was mentioned in section 2.4, it was necessary to supply the appropriate combination of tuning currents to the four sections of the laser to have a wavelength stable laser signal. Analog Devices have a good application note AN-1530, that shows how to implement high precision, low cost current sources using the difference amplifier AD8276 and the operational amplifier AD8603 for feedback loop.

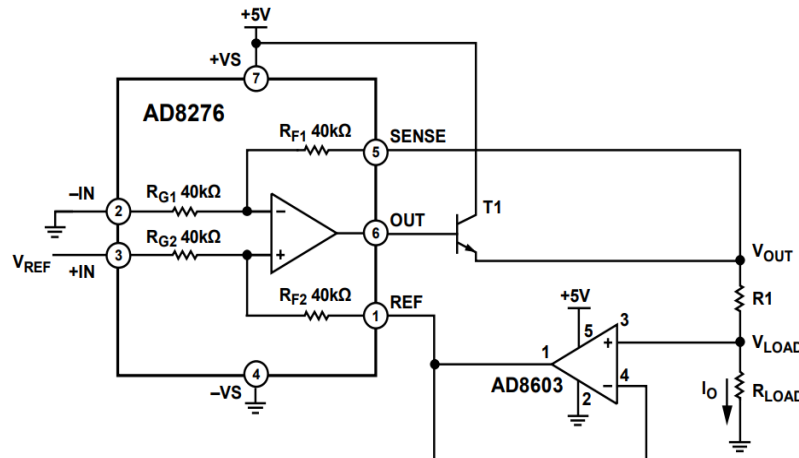


Figure 28. Current source with feedback loop



An input reference voltage,  $V_{ref}$ , is applied to the noninverting input of the difference amplifier. This voltage controls the amount of output current,  $I_O$ . The inverting input of the difference amplifier is connected directly to ground. There are four 40K $\Omega$  resistors inside the difference amplifier that are connected to the input pins, the REF pin and the SENSE pin. If the resistors are matched, the input reference voltage  $V_{ref}$  appears across the  $R_1$  resistor, producing output current,  $I_O$ , which can be calculated by using the following equation:

$$I_O = \frac{V_{ref} \left( \frac{R_{F2}}{R_{G2}} + \frac{R_{F1}}{R_{G1}} \cdot \frac{R_{F2}}{R_{G2}} \right)}{R_1 \left( 1 + \frac{R_{F2}}{R_{G2}} \right) + R_{LOAD} \left( \frac{R_{F2}}{R_{G2}} - \frac{R_{F2}}{R_{G2}} - \frac{R_{F1}}{R_{G1}} \right)} \quad (3)$$

Where  $R_{F1}$  and  $R_{F2}$  are feedback resistors and  $R_{G1}$  and  $R_{G2}$  are gain resistors. As the difference amplifier has resistor matching ( $R_{F1}/R_{G1} = R_{F2}/R_{G2} = 1$ , equation (3) can be simplified as:

$$I_O = \frac{V_{ref}}{R_1} \quad (3.1)$$

The accuracy of  $R_1$  is critical, so it must have  $\geq 0.1\%$  tolerance.

The operational amplifier is used in the feedback loop of the circuit and this model is chosen because of its low bias current (1 pA maximum) and offset voltage (less than 50  $\mu$ V). The low bias current makes possible to interface to a low impedance load without introducing significant offset errors.

The input range of the operational amplifier, the output range of the difference amplifier and the voltage range of the difference amplifier SENSE pin limit the amount of  $I_O$  available from the circuit.

It was designed a current source for each section of the laser, limiting the maximum current that the electrical characteristics says as shown in section 2.4. The maximum  $V_{ref}$  that can be obtained from the Red Pitaya analog outputs is 1.8V, so the only

thing it was necessary to calculate was the minimum resistance to limit the maximum current for each section according to the specifications from Table 1.

For gain section:

$$I_{G_{max}} = 150mA \quad (4)$$

$$\therefore R_{G_{min}} = \frac{V_{ref}}{I_{G_{max}}} = \frac{1.8V}{150mA} = 12\Omega \quad (4.1)$$

For coupler section:

$$I_{C_{max}} = 60mA \quad (5)$$

$$\therefore R_{C_{min}} = \frac{V_{ref}}{I_{C_{max}}} = \frac{1.8V}{60mA} = 30\Omega \quad (5.1)$$

For reflector section:

$$I_{R_{max}} = 50mA \quad (6)$$

$$\therefore R_{R_{min}} = \frac{V_{ref}}{I_{R_{max}}} = \frac{1.8V}{50mA} = 36\Omega \quad (6.1)$$

For phase section:

$$I_{P_{max}} = 10mA \quad (7)$$

$$\therefore R_{P_{min}} = \frac{V_{ref}}{I_{P_{max}}} = \frac{1.8V}{10mA} = 180\Omega \quad (7.1)$$

The four analog outputs of the Red Pitaya as voltage reference for each current source were used. Also, to have a feedback of the output voltage, the analog inputs of the Red Pitaya were implemented to measure the current sources.

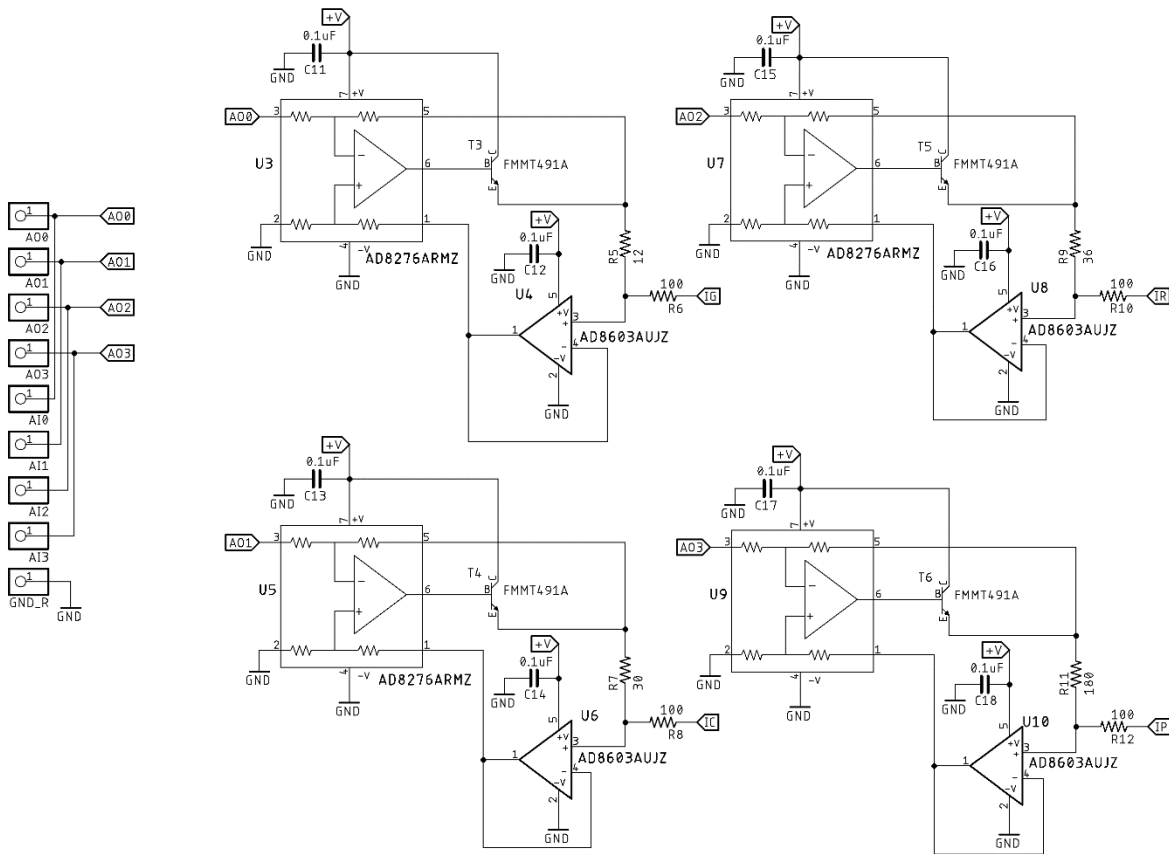


Figure 29. Current sources for each GCSR laser section.

### 3.2.1.3 TEMPERATURE CONTROLLER

This stage will be in charge of maintaining a constant temperature to the laser by controlling the thermoelectric cooler (TEC) and the thermistor. The temperature for the desired configuration with a trimmer can be manually fixed. It can be said that this stage was formed by two parts, a circuit that would measure the value of the thermistor and a circuit that would supply current to the TEC to reach the desired temperature for the laser.

The thermistor of the laser is NTC type (Negative Temperature Coefficient), that is, if the temperature increases, the resistance decreases. The R-T (Resistance-Temperature) curve of the thermistor is shown in Fig X.

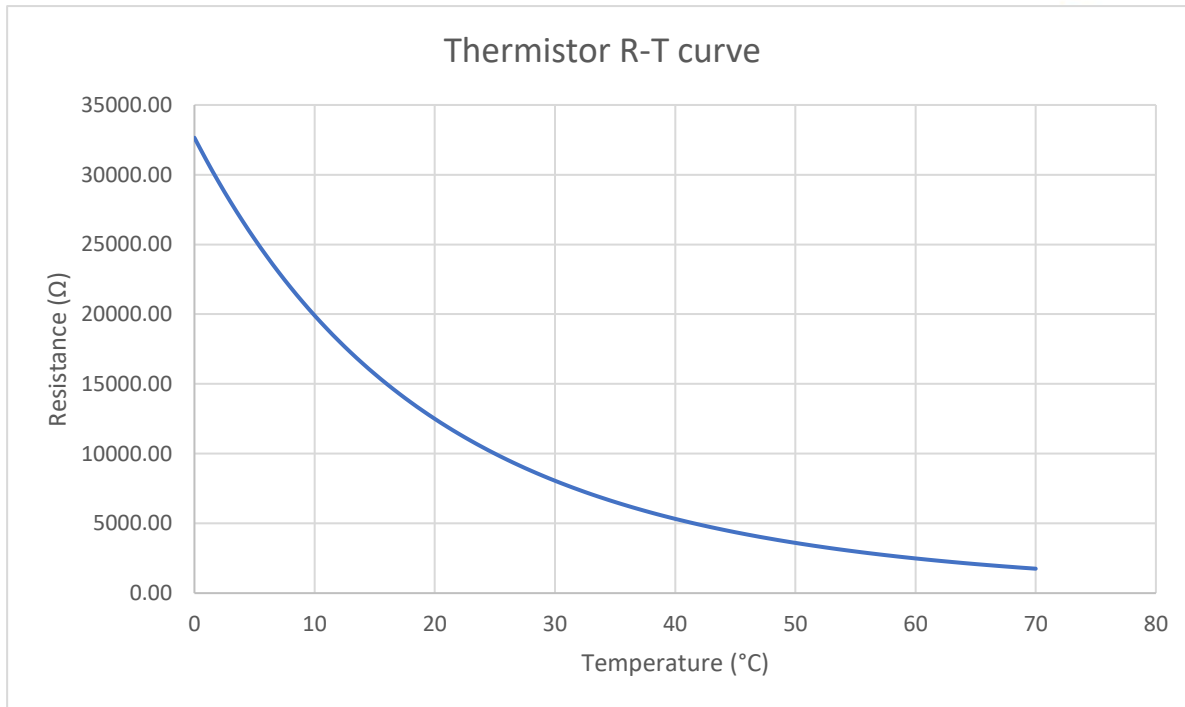


Figure 30. R-T curve of the thermistor.

The circuit that would read the value of the thermistor, was done by designing a Wheatstone bridge. The Wheatstone bridge circuit is nothing more than two simple series-parallel arrangements of resistances connected between a voltage supply terminal and ground producing zero voltage difference between the two parallel branches when balanced. This means that the bridge measures unknown resistances values. In this case, the unknown resistance is the thermistor. A Wheatstone bridge circuit has two input terminals and two output terminals consisting of four resistors configured in a diamond-like arrangement as shown in Fig. 17.

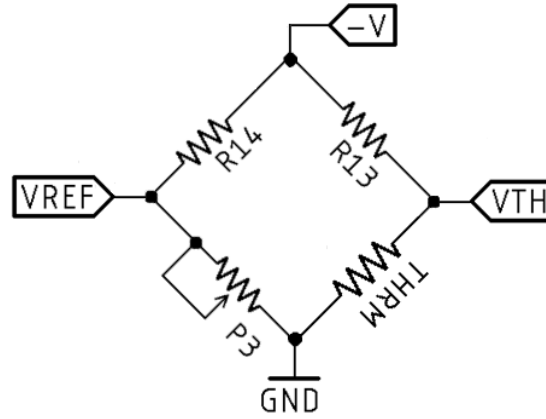


Figure 31. Wheatstone bridge circuit.

The bridge was connected between the negative voltage supply and ground.  $V_{ref}$  was the output of the voltage divider from  $R_{14}$  and  $R_{p3}$ . This voltage was used as temperature setpoint.  $V_{th}$  was the output of the voltage divider from  $R_{13}$  and  $R_{thrm}$ . This voltage gave the actual temperature of the laser. Their equations were:

$$V_{ref} = V_- \frac{R_{p3}}{R_{p3} + R_{14}} \quad (8)$$

$$V_{th} = V_- \frac{R_{thrm}}{R_{thrm} + R_{13}} \quad (9)$$

To find the error, it was necessary to subtract  $V_{th}$  to  $V_{ref}$ . For this, it was used a difference amplifier of unity gain. The output voltage of the difference amplifier was:

$$V_{error} = V_{ref} - V_{th} = V_- \left( \frac{R_{p3}}{R_{p3} + R_{14}} - \frac{R_{thrm}}{R_{thrm} + R_{13}} \right) \quad (10)$$

To have zero error,  $R_{p3}$  and  $R_{thrm}$  must be equal. The desired temperature was obtained when zero error was achieved.

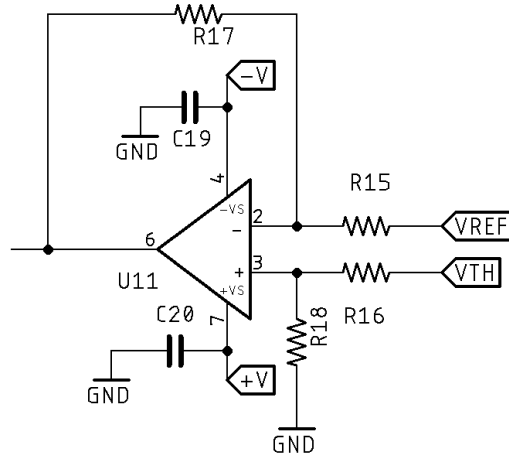


Figure 32. Voltage error.

The error generated in the Wheatstone bridge circuit was fixed by the second part of the temperature control, a PID controller.

A PID controller is a three-part system:

- Proportional

The main function of the proportional compensator is to introduce a gain that is proportional to the error reading which is produced by comparing the system's output and input. An inverting operational amplifier was used, as shown in Fig. 19:

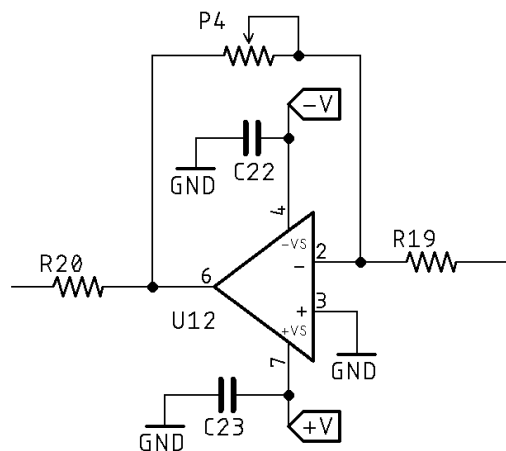


Figure 33. Proportional compensator.

- Derivative

This compensator will introduce the derivative of the error signal multiplied by a gain  $K_D$ . In other words, the slope of the error signal's waveform is what will be introduced to the output. Its main purpose is that of improving the transient response of the overall closed-loop system. It was used a high pass filter, as shown in Fig. 20:

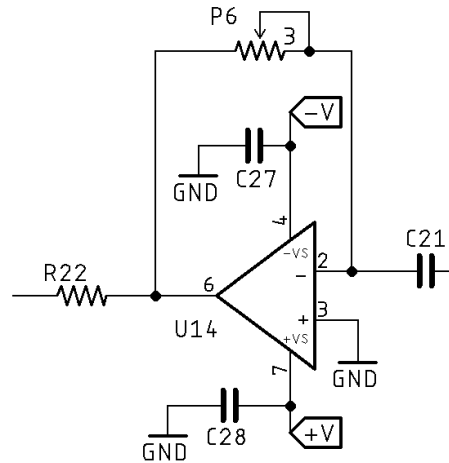


Figure 34. Derivative compensator.

- Integral

The compensator will introduce the integral of the error signal multiplied by a gain  $K_I$ . This means that the area under the error signal's curve will be affecting the output system. This facet of the controller will improve steady-state error of overall closed-loop system. It was used an integral compensator, as shown in Fig. 21:

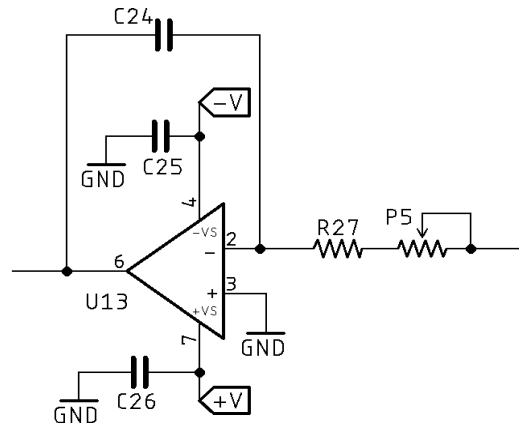


Figure 35. Integral compensator.

The response of the PID controller in the time domain is given by:

$$u(t) = K_P \left( e(t) + \frac{1}{T_i} \int_0^t e(\tau) d\tau + T_d \frac{de(t)}{dt} \right) \quad (11)$$

where  $u(t)$  is the control variable and  $e(t)$  is the control error. The PID controller is the sum of the three compensators. The controller parameters are: proportional gain  $K_P$ , integration time  $T_i$  and derivative time  $T_d$ . To find these parameters, many methods exist, but all of them imply to know the behaviour of the system to control. In this present case, the transient response of the laser temperature was measured and then the parameters were adjusted. The PID controller circuit is shown in Fig. 22.

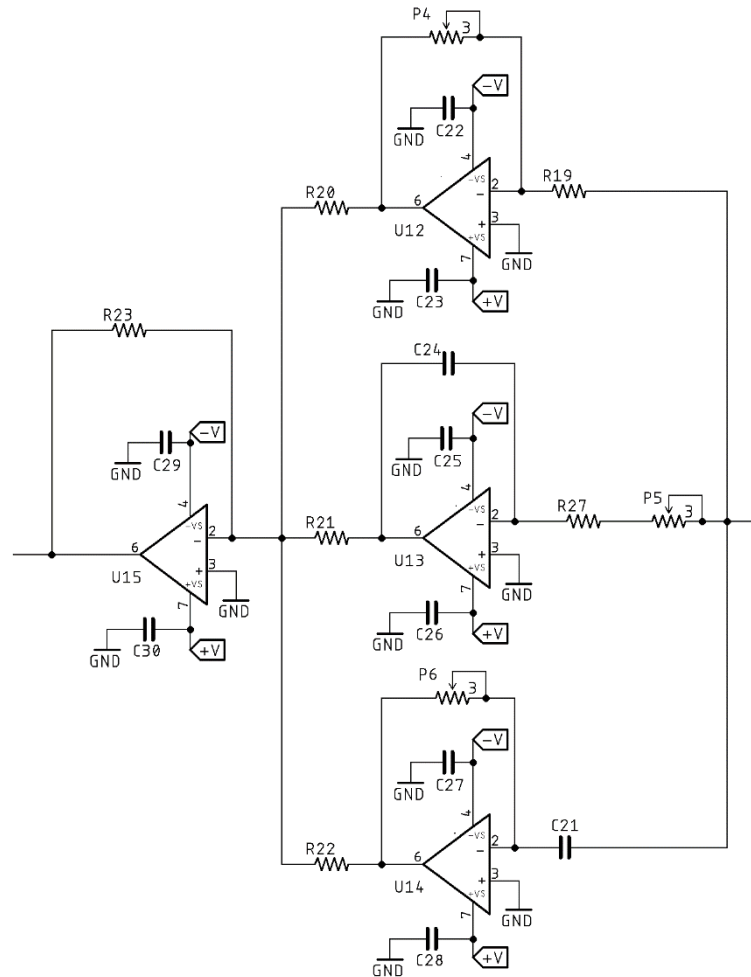


Figure 36. PID controller.



At the end of the PID controller, the current delivered from the summing op amp (around 25mA) was not enough for heating or cooling the laser, where the maximum current accepted by the TEC is 1.2A, as mentioned in Table 1. A Darlington amplifier stage was added to fix the problem. This current was controlled by resistance  $R_{26}$ , limiting the maximum current delivered in the TEC. For  $R_{26}$ ,  $3.3\Omega$  was chosen to have 1.03A as the maximum current injected to the TEC. It was also added an instrumentation amplifier to monitor the controller.

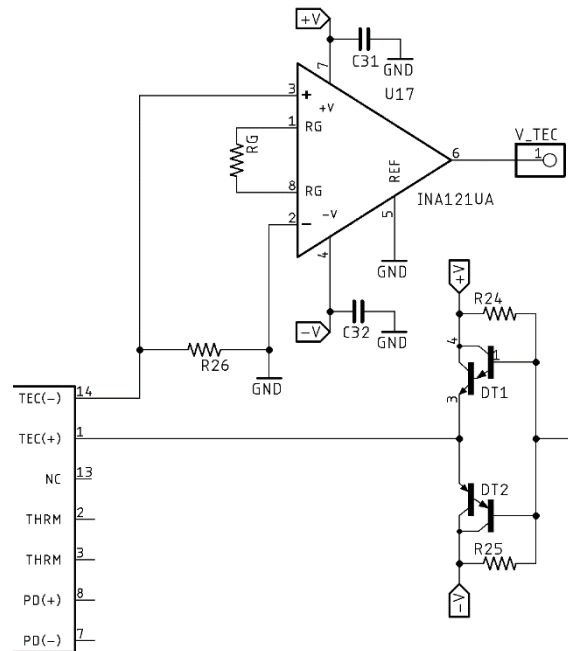


Figure 37. Darlington amplifier stage with current limit resistance and instrumentation amplifier.

### 3.2.1.4 OPTICAL MEASUREMENT

The laser has an internal photodiode, as seen in Fig. 8, that gets some radiation emitted from the laser directly. Therefore, it was used to measure the emitted optical power.

The photodiode generates a current proportional to the received radiation. To measure this current, it was converted to voltage by a linear relationship, and this could be achieved by using an inverting transimpedance stage.

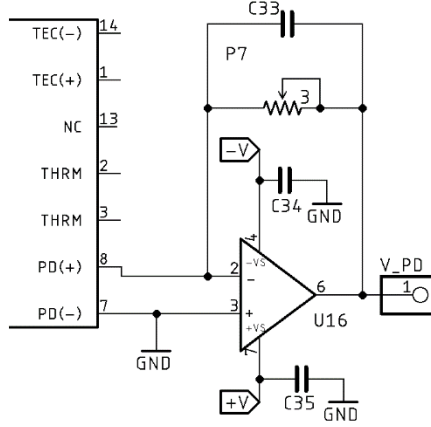


Figure 38. Inverting transimpedance stage measuring optical power

The expression of the output voltage of the inverting transimpedance amplifier is:

$$V_{PD} = R_{P7} \cdot I_{PD} = P_{PD} \cdot \mathfrak{R} \cdot R_{P7} \quad (12)$$

where  $P_{PD}$  is the output power of the photodiode,  $\mathfrak{R}$  is the responsivity (typically 0.85 A/V) and  $R_{P7}$  is the load resistor [9].

The gain of the stage is determined by the value of the resistance. The capacitor filters the noise that the signal has and together with the resistance it will set the output maximum frequency.

$$f = \frac{1}{2\pi \cdot R_{P7} \cdot C_{33}} \quad (13)$$

To choose the value of the capacitor, it was taken into account the following equation that relates the output voltage of the stage with the current that goes through the photodiode.

$$V_{PD} = I_{PD}(R_{P17} || Z_{C33}) \quad (14.1)$$

$$V_{PD} = I_{PD} \left( \frac{\frac{R_{P7}}{\omega C_{33}}}{R_{P7} + \frac{1}{\omega C_{33}}} \right) \quad (14.2)$$

$$V_{PD} = \frac{I_{PD} \cdot R_{P7}}{1 + \omega R_{P7} C_{33}} \quad (14.3)$$

Based on the equation (14.3), the value of the capacitor  $C_{33}$  was 220pF and the value of the resistance  $R_{P7}$  was determined by a trimmer, with a maximum value of 10KΩ. This means that the output maximum frequency can go from 72.34KHz to 723.43KHz. The conversion factor was given by the value of  $R_{P7}$ . For the testing,  $R_{P7}$  was set to 2.5kΩ, obtaining a conversion factor of 2.5 V/mA and an output maximum frequency of 289.37KHz.

To obtain the power,

### 3.2.2 COMPLETE CIRCUIT

Autodesk CADsoft EAGLE 8.7 was used. This is a program used for electronic and PCB design.

For the design, it was used SMD elements for the circuit, because they are economic, reduced in size and simple to mount. In the next figures the complete circuit: top and bottom sides of the designed PCB and the fabricated PCB can be seen.

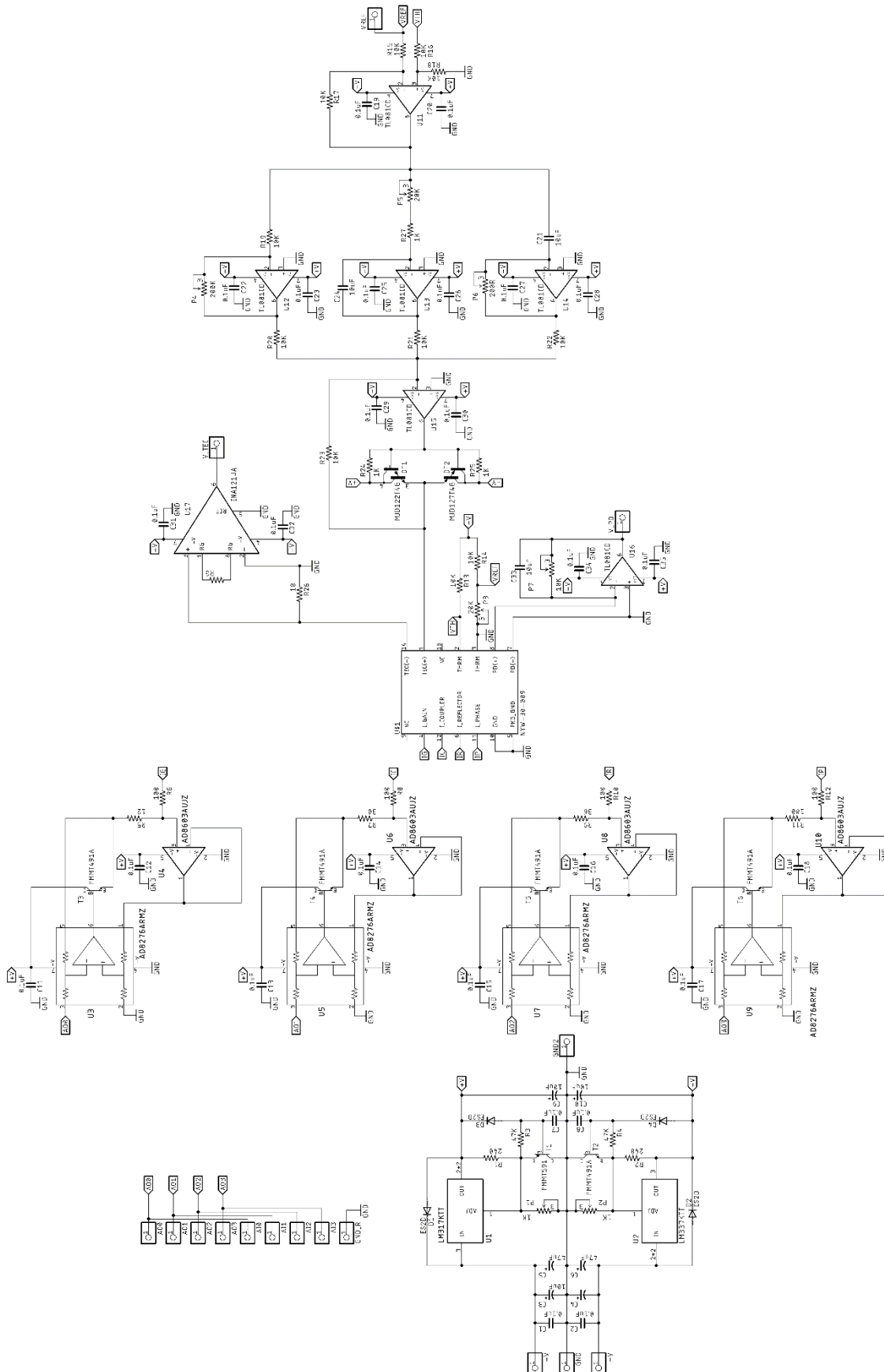


Figure 39. Complete circuit

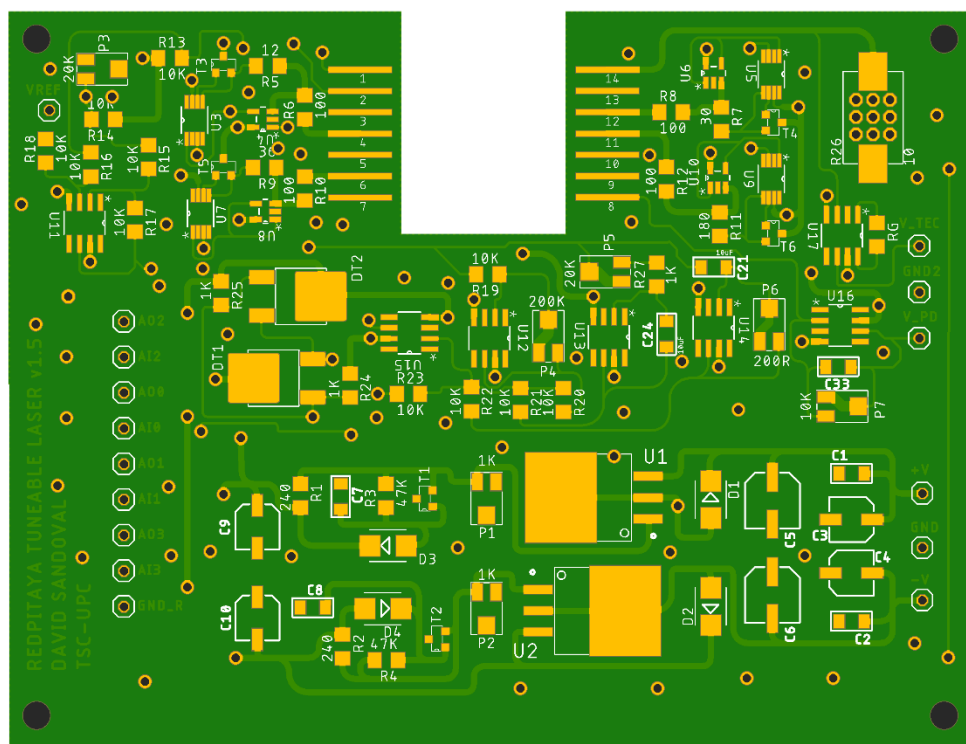


Figure 40. Top side of PCB.

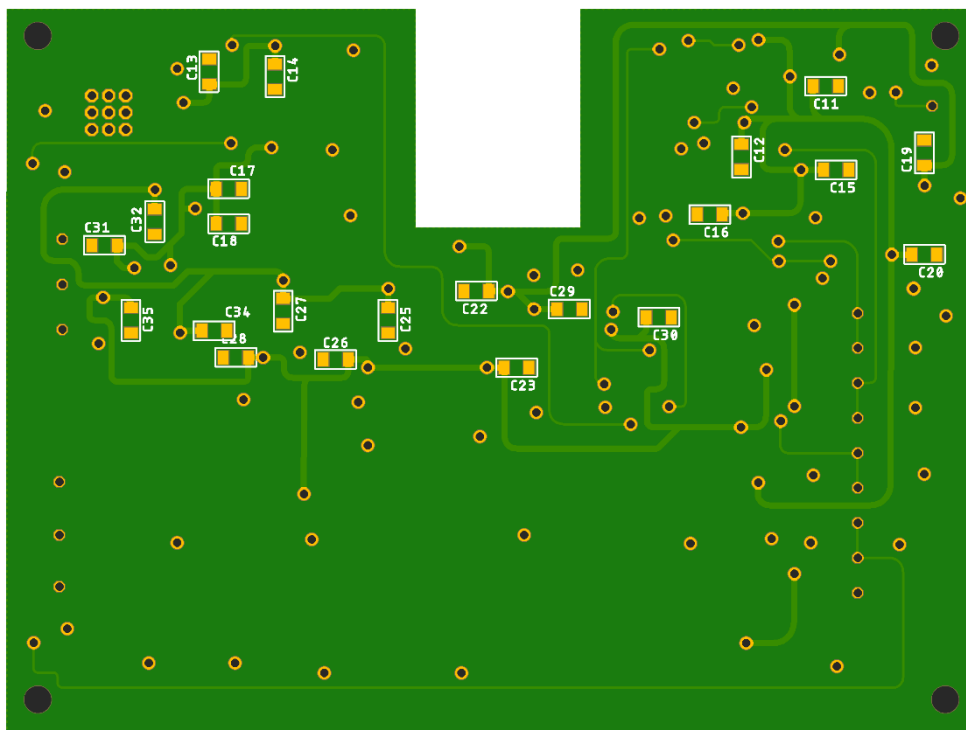


Figure 41. Bottom side of PCB.

### 3.3 INPUT OUTPUT RELATIONSHIP

Before starting the software design, it was necessary to establish the output voltages required for each section to tune the desired ITU channel. Once the current sources for each section of the laser were designed, the relationship could be established.

	$V_{Gain}$	$V_{Coupler}$	$V_{Reflector}$	$V_{Phase}$
<b><i>Output pin</i></b>	<b><i>A00</i></b>	<b><i>A01</i></b>	<b><i>A02</i></b>	<b><i>A03</i></b>

*Table 2. Physical output current correspondence*

### 3.4 SOFTWARE

#### 3.4.1 LANGUAGE SELECTION

As it was mentioned in section 2.5, it is possible to program the Red Pitaya using its SCPI server, with Matlab, Labview, Scilab or Python. From these four, the best languages that can be used to program the Red Pitaya are Matlab and Python. Programming is immensely important for data analysis. The following properties of a language are required:

- Ability of interactive sessions (it can help speed development)
- Linear algebra operations (matrix, vector operations)
- Quick and powerful graphing
- A large library of built-in functions (statistics, machine learning, etc)

Coming up next, the pros and cons of Matlab and Python for scientific computing will be summarized.

##### 3.4.1.1 Matlab

Matlab is an amazing product that helps to perform math-related tasks of all sorts using the same techniques that it would be used if the task were being performed

manually. Additionally, Matlab makes it possible to perform these tasks at a speed that only a computer can provide. In addition, using Matlab reduces errors, streamlines many tasks, and makes us more efficient. However, Matlab is also a big product that has a large number of tools and a significant number of features that might have never been used in the past. For example, instead of simply working with numbers, now we have the ability to plot them in a variety of ways that helps us to better communicate the significance of our data to other people.

Matlab has some definite benefits:

- Very polished Integrated Development Environment (IDE). We have a nice interactive workspace and a variable viewer in the main window. The editor has really become more modern in past years with nice features like auto-completion and variable highlighting.
- Big set of libraries. There seems to be an ever-expanding universe of toolboxes that do low-level tasks.
- Powerful graphing. There is a steep learning curve to learn to graph by code, but it is very powerful and easy once we understand it.
- Interaction with third party software.

But there are also drawbacks:

- Closed source. It is not always obvious how Matlab computes things.
- Expensive.

### 3.4.1.2 Python

Python is an example of a language that does everything right within the domain of things that it is designed to do. Programmers have been using Python so much that it is now the fifth-ranked language in the world. The amazing thing about Python is that an application can be written on one platform and used on every other platform that we need to support. Python emphasizes code readability and a concise syntax

that allows writing applications using fewer lines of code than other programming languages require.

Python has its strengths:

- Free.
- Open source.
- Powerful, full featured language.

But there are some drawbacks to Python:

- It is not as neatly packaged as Matlab.
- Engineers might not be as versed in Python as they are in Matlab.

### **3.4.1.3 Summary**

Matlab is a commercial numerical computing environment and programming language. The concept of Matlab refers to the whole package, including the IDE. The standard library does not contain much generic programming functionality but it does include matrix algebra and an extensive library for data processing and plotting. To do scientific computing in Python, you need additional packages. Also, you will need an IDE.

Matlab executes its programs more quickly, which means it can try more ideas and solve more complex problems. From the outset, Matlab is faster than Python for technical calculation tasks common in engineering calculations and data visualization.



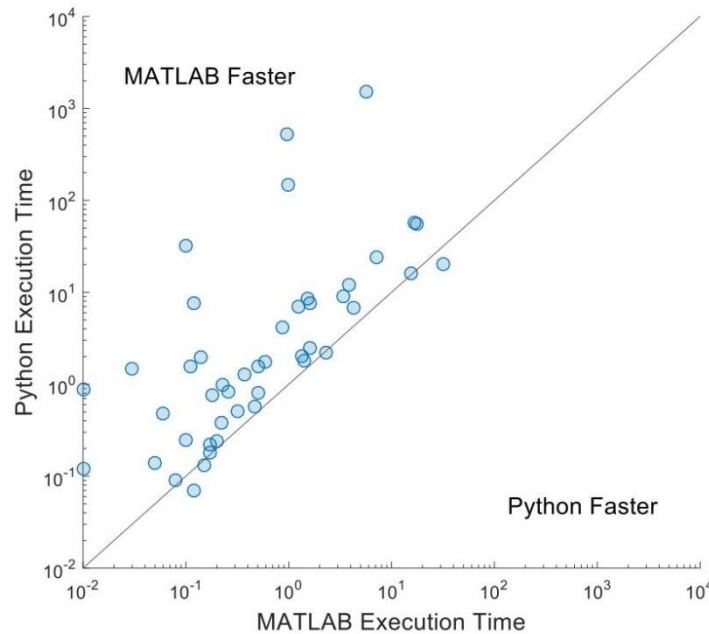


Figure 42. Comparison of Matlab and Python execution time for common technical computing tasks in statistics, engineering calculations, and data visualization. Each point represents the time of a single test run in each language [16].

Python code requires add-ons that overlap and conflict to obtain performance benefits such as just-in-time compilation and explicit parallel programming. These solutions tend to be incomplete or to be addressed to advanced programmers.

Python functions are usually designed and documented by advanced programmers for other experienced programmers. Python development environments for scientific calculation suffer from the reliability and integration of Matlab desktop.

Based on this, it was chosen to use Matlab, since its characteristics were more desirable for the project development.

### 3.4.2 MATLAB CODING

The main objective of the code is to control current sources to deliver an ITU channel by the GCSR laser. The relation established in section 3.3 is used as a database from where the program will obtain the voltage values. The user input will be just an ITU channel value.

The code structure is the following:

First, there is the startup, where the database to the program was loaded and the variables were cleared that were going to be used. Variable H stored the desired ITU channel and variable X located the values in the database for the selected ITU channel.

```
%% Startup

clc;
GCSR=readtable('GCSR.xlsx','ReadVariableNames',false);
H=0;
X=0;
```

*Figure 43. Startup.*

Next, it was defined the Red Pitaya as TCP/IP object and it was opened a connection between the SCPI server of the Red Pitaya and Matlab. In section 3.1 the steps to obtain the IP address are explained.

```
%% Define Red Pitaya as TCP/IP object

IP= '172.26.37.200';
port = 5000;
tcpipObj=tcpip(IP, port);

%% Open connection with your Red Pitaya

fopen(tcpipObj);
tcpipObj.Terminator = 'CR/LF';
```

*Figure 44. TCP/IP object definition and open connection*

Finally, it was implemented a while loop, to have constant output voltages. The code asks for the desired ITU channel. If the value is not between the channels (17 to 58), it gives a message that the ITU channel is not valid. If the requested channel is correct, then it starts delivering the necessary output voltages to tune it. The command window shows the ITU channel selected, the output voltage given with its related current, and voltage feedback of each output, so they can be monitored.

```
%% ITU channel selection

while H<59

    H=input('\n Insert ITU Channel(17 to 58) to deliver: ');

    if H<59

        X=H-16;

        clc

        G=GCSR(X,'Var2'); %%Gain voltage needed
        GA=G/12; %%Gain current delivered
        out_voltage0 = num2str(G);
        out_num0 = '0';
        scpi_command0 = strcat('ANALOG:PIN AOUT',out_num0,',',out_voltage0);
        fprintf(tcpipObj,scpi_command0);
        fprintf(' Gain Current = %.4f A \n',GA);
        fprintf(' \n Gain Output Voltage = %.4f V \n',G);
        volts0=str2double(query(tcpipObj,'ANALOG:PIN? AIN0')); %%Reads Gain voltage delivered
        fprintf(' \n Feedback Voltage = %.4f V \n \n ',volts0);

        C=GCSR(X,'Var3'); %%Coupler
        CA=C/30; %%Coupler current delivered
        out_voltage1 = num2str(C);
        out_num1 = '1';
        scpi_command1 = strcat('ANALOG:PIN AOUT',out_num1,',',out_voltage1);
        fprintf(tcpipObj,scpi_command1);
        fprintf(' \n Coupler Current = %.4f A \n',CA);
        fprintf(' \n Coupler Output Voltage= %.4f V \n',C);
        volts1=str2double(query(tcpipObj,'ANALOG:PIN? AIN1')); %%Reads Coupler voltage delivered
        fprintf(' \n Feedback Voltage = %.4f V \n \n ',volts1);

        R=GCSR(X,'Var4'); %%Reflector
        RA=R/36; %%Reflector current delivered
        out_voltage2 = num2str(R);
        out_num2 = '2';
        scpi_command2 = strcat('ANALOG:PIN AOUT',out_num2,',',out_voltage2);
        fprintf(tcpipObj,scpi_command2);
        fprintf(' \n Reflector Current = %.4f A \n',RA);
        fprintf(' \n Reflector Output Voltage= %.4f V \n',R);
        volts2=str2double(query(tcpipObj,'ANALOG:PIN? AIN2')); %%Reads Reflector voltage delivered
        fprintf(' \n Feedback Voltage = %.4f V \n \n ',volts2);

        P=GCSR(X,'Var5'); %%Phase
        PA=P/180; %%Phase current delivered
        out_voltage3 = num2str(P);
        out_num3 = '3';
        scpi_command3 = strcat('ANALOG:PIN AOUT',out_num3,',',out_voltage3);
        fprintf(tcpipObj,scpi_command3);
        fprintf(' \n Phase Current = %.4f A \n',PA);
        fprintf(' \n Phase Output Voltage= %.4f V \n',P);
        volts3=str2double(query(tcpipObj,'ANALOG:PIN? AIN3')); %%Reads Phase voltage delivered
        fprintf(' \n Feedback Voltage = %.4f V \n \n ',volts3);

        elseif H>58

            fprintf('\n The desired ITU Channel is not valid \n \n');

            break

        elseif H<17

            fprintf('\n The desired ITU Channel is not valid \n \n');

            break

        end

    end

end

%%
```

Figure 45. ITU channel selection.

## CHAPTER 4

### TESTING AND RESULTS

#### 4.1 ASSEMBLING AND RUNNING PROJECT

Once the PCB board was fabricated, all the components of the circuit were soldered and the next step was the experimental verification of its functioning.

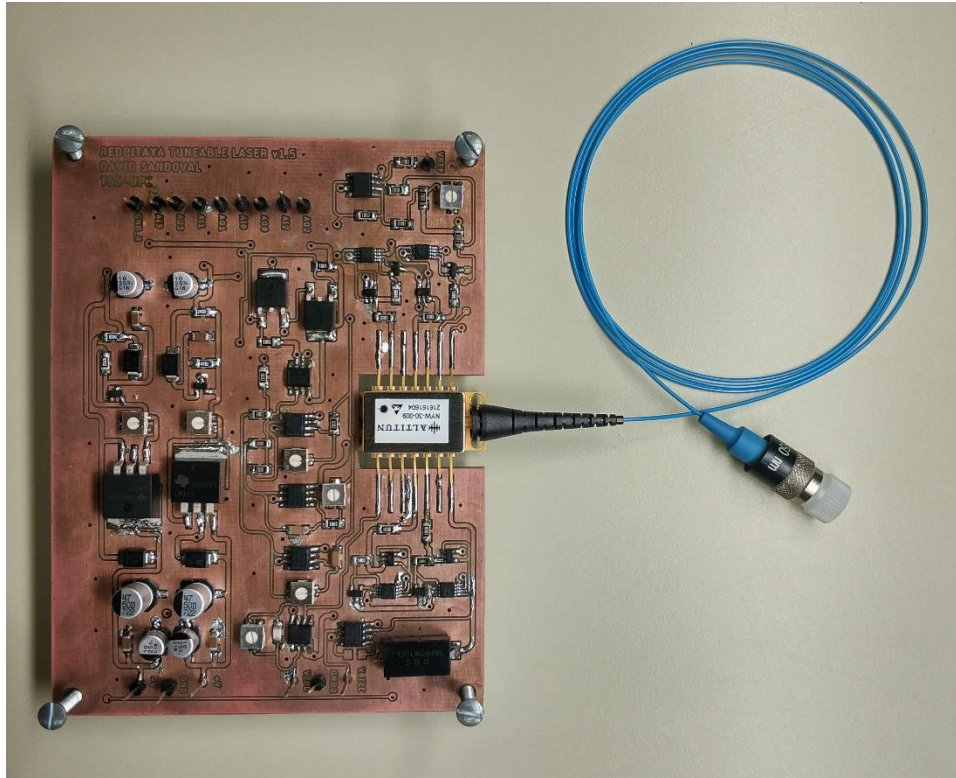


*Figure 46. PCB board mounted*

Before running the program, the hardware was setup by connecting the Red Pitaya extension connector to the input pins of the PCB board. The corresponding pins are written in the board. To read the output of the laser, the FC connector was connected to an FTB-2 optical spectrum analyser.

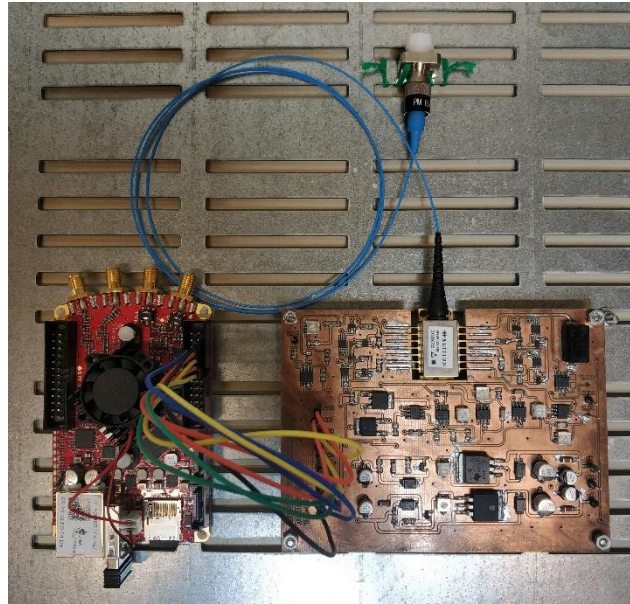


Figure 47. Hardware setup

As mentioned in section 3.1, it was necessary to take into account the output voltage error of the Red Pitaya, so the input-output table was updated manually by test-error to assure perfect matching.

All the ITU channels were successfully tuned with a maximum error of 0.01%, but some of the tuned channels were not completely clean, obtaining more than 42dB of side-mode suppression ratio (SMSR), where the typical is 35dB, according to the laser specifications.

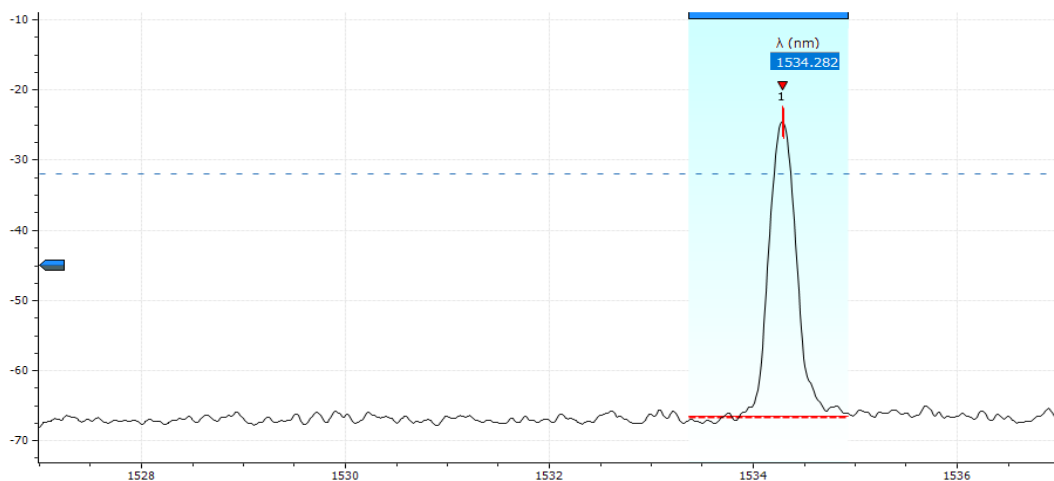


Figure 48. ITU Channel 54 spectrum

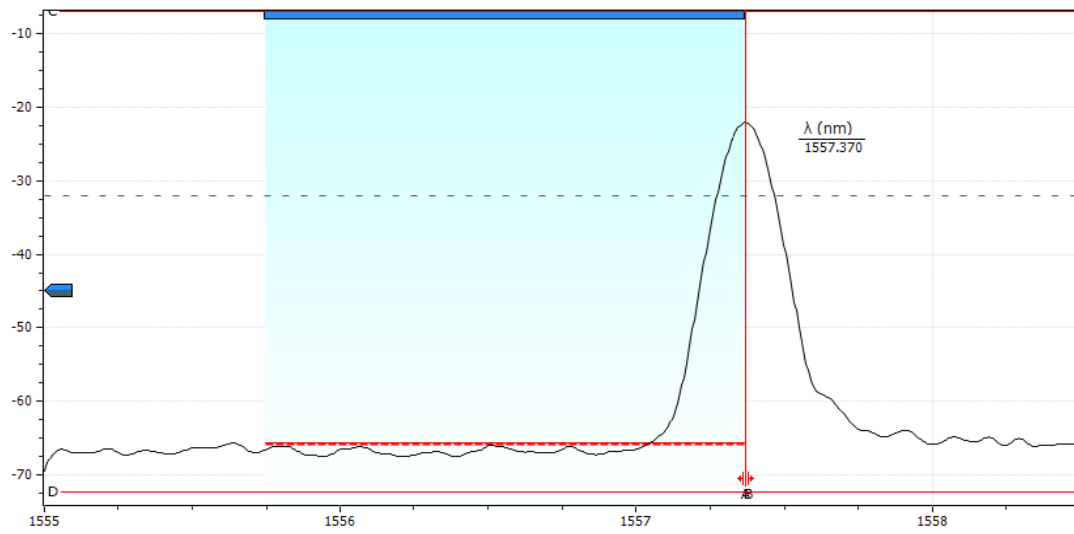


Figure 49. ITU Channel 25 spectrum



Figure 50. ITU Channel 30 spectrum

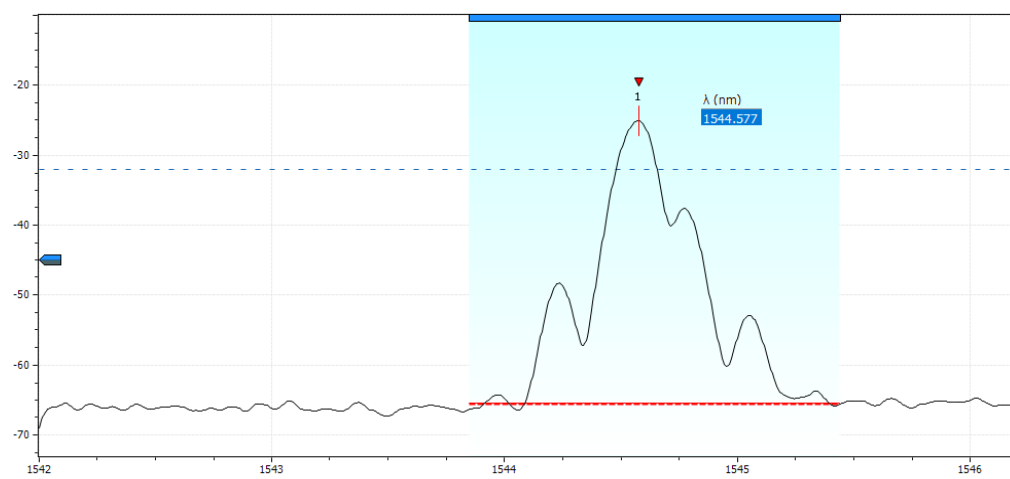


Figure 51. ITU Channel 41 spectrum



In Table 5 we updated the values of the currents of each section with their corresponding voltage for a temperature of 25°C.

ITU Channel	$f$ (THz)	$\lambda_{ITU}$ (nm)	$\lambda_{Channel}$ (nm)	$I_{Gain}$ (mA)	$I_{Coupler}$ (mA)	$I_{Reflector}$ (mA)	$I_{Phase}$ (mA)	$P_{OUT}$ (dBm)	$V_{Gain}$ (V)	$V_{Coupler}$ (V)	$V_{Reflector}$ (V)	$V_{Phase}$ (V)
17	191.7	1563.86	1563.841	100	6.33	37.22	5.5	-2.95	1.23	0.19	1.34	0.99
18	191.8	1563.05	1563.036	100	6.33	41.67	2.22	-1.83	1.23	0.19	1.5	0.4
19	191.9	1562.23	1562.234	100	7.67	19.44	2.22	0.38	1.23	0.23	0.7	0.4
20	192	1561.42	1561.425	100	7.67	27.77	3.33	-0.41	1.23	0.23	1	0.6
21	192.1	1560.61	1560.624	100	8.33	30.55	1.11	0.05	1.23	0.25	1.1	0.2
22	192.2	1559.79	1559.793	100	8.33	33.33	3.33	-0.85	1.23	0.25	1.2	0.6
23	192.3	1558.98	1558.941	100	8.33	36.67	0.55	-1.09	1.23	0.25	1.32	0.1
24	192.4	1558.17	1558.214	100	8.33	41.67	2.22	-1.98	1.23	0.25	1.5	0.4
25	192.5	1557.36	1557.37	100	8.67	20.83	3.33	-0.45	1.23	0.26	0.75	0.6
26	192.6	1556.55	1556.562	100	8.67	27.77	2.77	-0.56	1.23	0.26	1	0.5
27	192.7	1555.75	1555.73	100	8.67	31.38	6.67	-1.42	1.23	0.26	1.13	1.2
28	192.8	1554.94	1554.978	100	8.67	33.33	3.33	-1.49	1.23	0.26	1.2	0.6
29	192.9	1554.13	1554.13	100	8.67	36.94	6.67	-1.83	1.23	0.26	1.33	1.2
30	193	1553.33	1553.322	100	8.67	40.83	1.11	-1.7	1.23	0.26	1.47	0.2
31	193.1	1552.52	1552.554	100	9.67	13.88	3.33	-0.12	1.23	0.29	0.5	0.6
32	193.2	1551.72	1551.7	100	9.67	28.05	3.33	-0.59	1.23	0.29	1.01	0.6
33	193.3	1550.92	1550.917	100	9.67	30.27	3.61	-0.54	1.23	0.29	1.09	0.65
34	193.4	1550.12	1550.121	100	9.67	33.33	1.67	-1.01	1.23	0.29	1.2	0.3
35	193.5	1549.32	1549.402	100	10.33	36.11	3.33	-1.66	1.23	0.31	1.3	0.6
36	193.6	1548.51	1548.554	100	11.67	5.55	2.22	-2.35	1.23	0.35	0.2	0.4
37	193.7	1547.72	1547.729	100	11.67	25.27	6.11	-1.22	1.23	0.35	0.91	1.1
38	193.8	1546.92	1546.917	100	11.67	27.77	2.22	-0.73	1.23	0.35	1	0.4
39	193.9	1546.12	1546.155	100	11.67	30.55	3.33	-1.18	1.23	0.35	1.1	0.6
40	194	1545.32	1545.23	100	12	38.05	7.77	-2.52	1.23	0.36	1.37	1.4
41	194.1	1544.53	1544.577	100	11.67	36.11	0.62	-1.92	1.23	0.35	1.3	0.62
42	194.2	1543.73	1543.629	100	13.33	25	3.33	-1.47	1.23	0.4	0.9	0.6
43	194.3	1542.94	1542.812	100	12.33	9.72	3.33	-2.6	1.23	0.37	0.35	0.6
44	194.4	1542.14	1542.177	100	13.33	27.77	1.11	-0.32	1.23	0.4	1	0.2
45	194.5	1541.35	1541.423	100	13.33	30.55	3.33	-1.44	1.23	0.4	1.1	0.6
46	194.6	1540.56	1540.587	100	13.33	33.61	1.11	-1.15	1.23	0.4	1.21	0.2
47	194.7	1539.77	1539.765	100	13.33	36.67	1.11	-1.6	1.23	0.4	1.32	0.2
48	194.8	1538.98	1538.802	100	16.33	13.88	2.22	-0.26	1.23	0.49	0.5	0.4
49	194.9	1538.19	1538.127	100	15	5.55	0.55	-0.68	1.23	0.45	0.2	0.1
50	195	1537.4	1537.442	100	16.67	2.77	2.22	-1.66	1.23	0.5	0.1	0.4
51	195.1	1536.61	1536.698	100	13.33	26.11	4.44	-1.52	1.23	0.4	0.94	0.8
52	195.2	1535.82	1535.94	100	15.33	33.33	2.22	-2.32	1.23	0.46	1.2	0.4
53	195.3	1535.04	1535.085	100	15.67	33.88	5	-2.34	1.23	0.47	1.22	0.9
54	195.4	1534.25	1534.282	100	18.33	8.33	3.33	-2.7	1.23	0.55	0.3	0.6
55	195.5	1533.47	1533.42	100	20	28.33	5	-2.22	1.23	0.6	1.02	0.9
56	195.6	1532.68	1532.68	100	20	30	5	-2.35	1.23	0.6	1.08	0.9
57	195.7	1531.9	1531.925	100	21	32.77	2.22	-2.7	1.23	0.63	1.18	0.4
58	195.8	1531.12	1531.111	100	20	35.83	3.33	-2.75	1.23	0.6	1.29	0.6

Table 3. Input output relationship updated

## CHAPTER 5

### BUDGET

In Table 5 we can see the total cost of the project, with the Bill of Materials and man power cost.

#	Item	Quantity	Unitary cost w/o taxes	Taxes per unit	Unitary cost with taxes	Total
1	Ceramic Capacitor SMD 0.1uF 1206	26	0.545	0.136	0.681	17.706
2	Ceramic Capacitor SMD 220pF 1206	1	0.558	0.139	0.697	0.697
3	Ceramic Capacitor SMD 10uF 1206	3	0.808	0.202	1.01	3.03
4	Electrolytic Capacitor SMD 47uF 6.7mm	2	0.250	0.062	0.312	0.624
5	Electrolytic Capacitor SMD 10uF 5mm	4	0.236	0.059	0.295	1.18
6	Resistor SMD 1206 240R	2	0.066	0.016	0.082	0.164
7	Resistor SMD 1206 47K	2	0.066	0.016	0.082	0.164
8	Resistor SMD 1206 12R	2	0.066	0.016	0.082	0.164
9	Resistor SMD 1206 30R	2	0.066	0.016	0.082	0.164
10	Resistor SMD 1206 36R	2	0.066	0.016	0.082	0.164
11	Resistor SMD 1206 180R	2	0.066	0.016	0.082	0.164
13	Resistor SMD 1206 10K	11	0.066	0.016	0.082	0.902
14	Resistor SMD 1206 1K	2	0.066	0.016	0.082	0.164
15	Resistor SMD SMW5 10R	1	0.669	0.167	0.836	0.836
17	Potentiometer SMD 1K	2	1.368	0.342	1.71	3.42
18	Potentiometer SMD 20K	2	1.368	0.342	1.71	3.42
20	Potentiometer SMD 200K	1	1.368	0.342	1.71	1.71
21	Potentiometer SMD 500R	1	1.368	0.342	1.71	1.71
22	Potentiometer SMD 10K	1	1.368	0.342	1.71	1.71
23	ES2D Rectifier Diode	4	0.466	0.116	0.582	2.328
24	FMMT491TA NPN Bipolar Transistor	5	0.289	0.072	0.361	1.805
25	FMMT591 PNP Bipolar Transistor	1	0.289	0.072	0.361	0.361
26	MJD122T4G NPN Darlington	1	0.381	0.095	0.476	0.476
27	MJD127T4G PNP Darlington	1	0.453	0.113	0.566	0.566
28	LM317KTT Voltage regulator	1	0.551	0.138	0.689	0.689
29	LM337KTT Voltage regulator	1	0.888	0.222	1.11	1.11
30	AD8276ARMZ	4	1.808	0.452	2.26	9.04
31	AD8603AUJZ	4	1.080	0.270	1.35	5.4
32	TL081CD Operational Amplifier	6	0.354	0.089	0.443	2.658
33	INA121 Instrumentation Amplifier	1	4.880	1.220	6.1	6.1
34	NYW-30-009 GCSR Laser	1	800.000	200.000	1000	1000
35	Cable to Board Header	1	1.696	0.424	2.12	2.12
36	PCB board	1	15.92	3.98	19.90	19.90
37	Manpower cost	750	8.000	2.000	10	7500
<b>TOTAL</b>						<b>8590.646</b>

Table 4. Project budget



## CHAPTER 6

### CONCLUSIONS AND FUTURE DEVELOPMENTS

In this project, a functional Red Pitaya system to control a tuneable laser has been created reducing the setting of the ITU channel to introducing the desired channel. This satisfies the requirement of presenting a transparent input-output relationship for the user and converts the channel tuning into an easy and fast process.

A limitation of this project is that the designed circuit has to be connected to an external power supply, because the power supplies of the Red Pitaya have a current limit of 500mA and are mostly used by the DAC. Also, with the resistances of the current sources there is a big span of the permitted current, but the size of the voltage steps increases, making the tuning less precise, and dangerous because allowed values can be exceeded. Once the characterization of the laser is done, the resistance of each section can be changed so that the maximum current delivered is the highest value obtained from each one.

Another limitation is that the prototype and database is specific for the stated laser model. To make this prototype compatible with other tuneable lasers, these two limitations should be eliminated. The resistances of the current sources should be changed every time and that's why it should be considered testing a variable resistor in the current source.

With the mentioned additions to the prototyped circuit of this project, if possible, there would be a complete adaptable circuit to supply different models of tuneable lasers.

## BIBLIOGRAPHY

- [1] V. M. P. Querol, "Contribution to the dynamic tuning of tunable laser sources for modulation and optical packet routing in WDM and access networks", Universitat Politècnica de Catalunya, 2006.
- [2] I. R. Smolinska, "DAC development with Raspberry Pi for future tunable laser application", Universitat Politècnica de Catalunya, 2017.
- [3] Y. Fukashiro, K. Sgrikhande, M. Avenarius, M. S. Rogge, I. M. White, D. Wonglumson and L. G. Kazovsky, "Fast and fine wavelength tuning of a GCSR laser using a digitally controlled driver," pàgs. 338-340, OFC 2000.
- [4] STEMLab Red Pitaya documents: <http://redpitaya.readthedocs.io/en/latest/>
- [5] Analog Devices, "High Precision, Low Cost Current Sources Using the AD8276 Difference Amplifier and the AD8603 Op Amp", Application Note AN-1530.
- [6] A. Díaz-Conti Escribano, "Diseño y caracterización de un circuito de acondicionamiento de un láser DFB para su aplicación en redes ópticas de acceso y metropolitanas", Universidad de Zaragoza, 2015.
- [7] Tube filament / header soft start: <http://www.diy-audio-guide.com/soft-start.html>
- [8] Aaron Dahlen, "The PID Controller series":  
[http://www.nutsvolts.com/magazine/article/the\\_pid\\_controller\\_part\\_1](http://www.nutsvolts.com/magazine/article/the_pid_controller_part_1)
- [9] Thorlabs Photodiode tutorial:  
[https://www.thorlabs.com/newgrouppage9.cfm?objectgroup\\_id=9020](https://www.thorlabs.com/newgrouppage9.cfm?objectgroup_id=9020)
- [10] F.J. Duarte, "Tunable lasers applications", 2<sup>nd</sup> Edition, CRC Press, 2009.
- [11] J.A. Altabas, D. Izquierdo, J.A. Lázaro & I. Garcés, "Chirp-based direct phase modulation of VCSELs for cost-effective transceivers", Optics letters, 42(3), 583-586, 2017.
- [12] G.L. Li, P.K.L. Yu, "Optical intensity modulators for digital and analog applications", Journal of Lightwave Technology, 21(9), 2010.
- [13] A. Yariv, "Optical electronics in modern communications", Oxford Series in Electrical and Computer Engineering, 1997.
- [14] J. Buus & E.J. Murphy, "Tunable lasers in optical networks", Journal of Lightwave Technology, 24(1), 5, 2006.
- [15] L.A. Coldren, G.A. Fish, Y. Akulova, J.S. Barton, L. Johansson & C.W. Coldren, "Tunable semiconductor lasers: A tutorial", Journal of Lightwave Technology, 22(1), 193, 2004.

[16] Main reasons to choose Matlab:

<https://es.mathworks.com/products/matlab/matlab-vs-python.html>

## GLOSSARY

<b>GCSR</b>	Grating assisted Coupler with Sampled Rear-reflector
<b>PCB</b>	Printed Circuit Board
<b>ITU</b>	International Telecommunications Union
<b>SCPI</b>	Standard Commands for Programmable Instruments
<b>USB</b>	Universal Serial Bus
<b>IP</b>	Internet Protocol
<b>DAC</b>	Digital to Analog Converter
<b>TEC</b>	Thermo-Electric Cooler
<b>PID</b>	Proportional-Integral-Derivative
<b>SMD</b>	Surface Mount Device
<b>FC</b>	Fiber Channel
<b>IDE</b>	Integrated Development Environment